Functional Neuroanatomy

Thomas P. Naidich and Tarek A. Yousry

Contents

T.P. Naidich
Mount Sinai School of Medicine,
One Gustave Levy Place, New York, NY 10029-6574, USA

Department of Neuroradiology and Neurosurgery,
Irving and Dorothy Regenstreif Research, New York, NY, USA

T.A. Yousry (✉)
Lysholm Department of Neuroradiology,
The National Hospital for Neurology and Neurosurgery,
Institute of Neurology, Queen Square, London WC1N 3BG, UK
e-mail: t.yousry@ucl.ac.uk

Abstract

We present the surface anatomy of the brain describing in detail the typical configuration of the sulci and gyri and their most frequent variations. After describing the borders of the lobes, we give guidance on the methods of localizing functionally important atomic structures such as the pericentral cortex, Heschl's gyrus, and the calcarine sulcus.

On the basis of the surface anatomy and the cytoarchitectonic subdivision of the cortex, we describe the function of selected areas related to the motor system and to speech.

1 Introduction

Modern neurophysiology and fMRI have refined our concepts of cerebral organization. This section presents the surface anatomy of the brain and begins to addresses the functional interrelationships among the cortical areas.

2 Surface Anatomy

2.1 Convexity Surface

2.1.1 Sylvian Fissure

The convexity face of the sylvian fissure displays five major arms (rami) that help to define the surface anatomy of the convexity (Fig. 1). The long nearly horizontal portion of the sylvian fissure is the posterior horizontal ramus. At its anterior end, the anterior horizontal ramus and the anterior ascending ramus arise together in a "V" or "Y" configuration. At its posterior end, the prominent posterior ascending ramus and the small posterior descending ramus branch outward in a "T" or "fishtail" configuration. The anterior subcentral sulcus and the posterior subcentral sulcus form two minor arms that extend superiorly into the frontoparietal operculum to delimit the subcentral gyrus. One or multiple
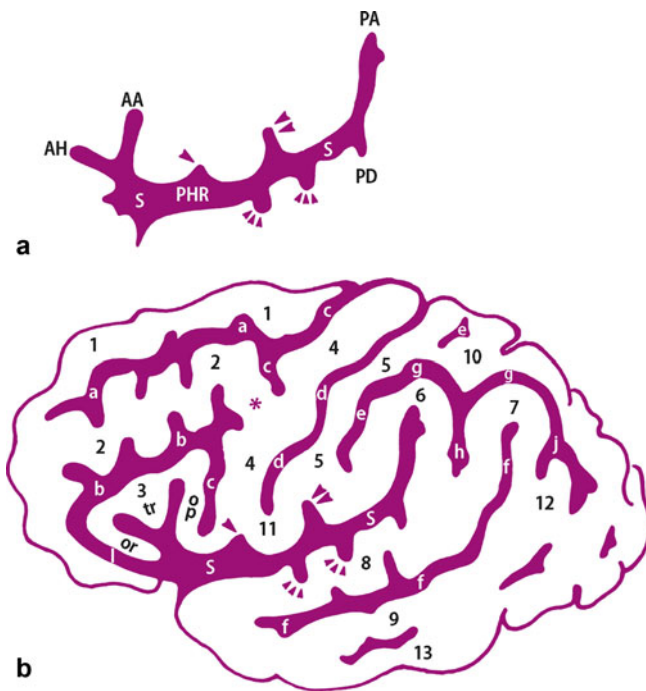
Fig. 1 (**a**, **b**) Surface anatomy of the convexity. (**a**) Sylvian fissure (*dark area*). The margins of the frontal, parietal, and temporal opercula are defined by the configuration of the sylvian fissure (*S*), its five major rami (the anterior horizontal ramus (*AH*), anterior ascending ramus (*AA*), posterior horizontal ramus (*PHR*), posterior ascending ramus (*PA*), and posterior descending ramus (*PD*), and its minor arms, the anterior subcentral sulcus (*single arrowhead*), posterior subcentral sulcus (*double arrowheads*), and transverse temporal sulci (*triple arrowheads*). (**b**) Cerebral convexity. The configuration of the sylvian fissure then permits identification of the adjoining gyri and sulci. GYRI: *1* superior frontal gyrus (*SFG*), *2* middle frontal gyrus (*MFG*), *3* inferior frontal gyrus (or, pars orbitalis; tr, pars triangularis; op, pars opercularis), *4* precentral gyrus (*preCG*), *5* postcentral gyrus (*post CG*), *6* supramarginal gyrus (*SMG*), *7* angular gyrus (*AG*), *8* superior temporal gyrus (*STG*), *9* middle temporal gyrus (*MTG*), *10* superior parietal lobule (*SPL*), *11* subcentral gyrus, *12* temporo-occipital arcus, *13* inferior temporal gyrus: * union of the MFG (*2*) with the preCG (*4*). SULCI; *a* superior frontal sulcus (*SFS*), *b* inferior frontal sulcus (*IFS*), *c* precentral sulcus (*preCS*), *d* central sulcus (*CS*), *e* postcentral sulcus (*post CS*), *f* superior temporal sulcus (*STS*), *g* intraparietal sulcus (*IPS*), *h* primary intermediate sulcus, *j* secondary intermediate sulcus, *k* accessory intermediate sulcus (not shown in this image), *S* sylvian fissure, *single black arrowhead* anterior subcentral sulcus, *double black arrowheads* posterior subcentral sulcus, *triple black arrowheads* transverse temporal sulci. Note specifically how the anterior horizontal and anterior ascending rami of the sylvian fissure divide the inferior frontal gyrus into the three partes orbitalis (*or*), triangularis (*tr*), and opercularis (*op*). The lateral orbital sulcus (*l*) separates the pars orbitalis from the lateral orbital gyrus (From Naidich et al. (1995); with permission)

Fig. 2 (**a–c**) Normal cerebral convexity. (**a**) Anatomic specimen full surface. (**b**) Magnified view of the low-middle convexity. (**c**) Magnified oblique view of the parietal lobe. The surface vessels and the pia-arachnoid have been removed to expose the gyri and sulci more clearly (labels as in Fig. 1.). In (**a**), the *single large white arrowhead* = preoccipital notch. In (**b**), the portions of the sylvian fissure (*S*) are indicated: *first white S* = vallecula leading to the anterior horizontal ramus (*single white arrow*) and the anterior ascending ramus (*double white arrow*); *second white S* = posterior horizontal ramus; *third white S* = posterior ascending ramus; *short black arrow* = posterior descending ramus of the sylvian fissure. In (**c**), the anterior border of the occipital lobe extends from the lateral end of the parieto-occipital sulcus (*large white arrow*) above to the preoccipital notch (*large white arrowhead*) below. The intraparietal sulcus (*multiple large black arrows*) crosses the theoretical lobar border to become the intraoccipital sulcus (*multiple large white arrows*). The inferior parietal lobule is composed of the SMG (*6*), the AG (*7*), and the temporo-occipital arcus (second *pli de passage* of Gratiolet) (*12*). The superior parietal lobule merges into the superior occipital gyrus across the parieto-occipital border through the parieto-occipital arcus (first *pli de passage* of Gratiolet) (*14*) (**a**, **b** from Naidich et al. (1997); (**c**) From Naidich and Brightbill (1995); with permission)

transverse temporal sulci extend inferiorly into the temporal lobe in relation to the transverse temporal gyrus of Heschl.

2.1.2 Frontal Lobe

The convexity surface of the frontal lobe is formed by four gyri and three sulci (Fig. 2). The superior frontal gyrus (SFG) is a horizontally oriented, roughly rectangular bar of tissue that forms the uppermost margin of the frontal lobe. The middle frontal gyrus (MFG) is a horizontally oriented, undulant length of tissue that zigzags posteriorly to merge with the anterior face of the precentral gyrus. The
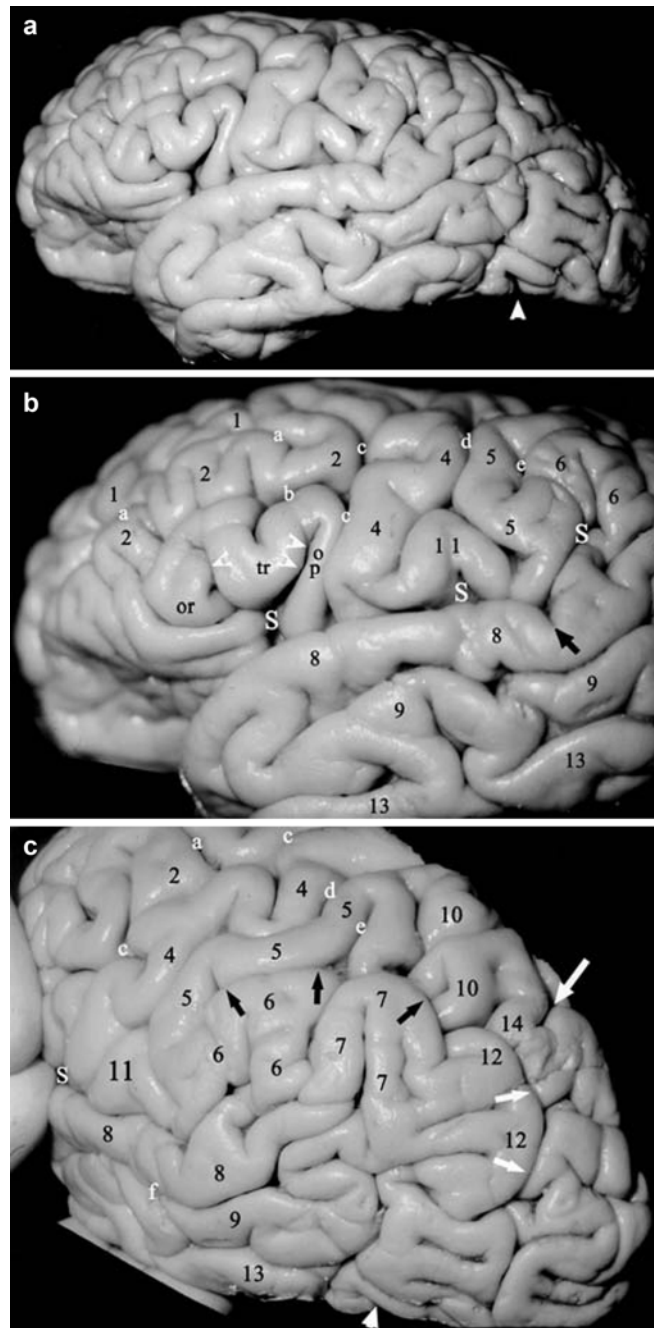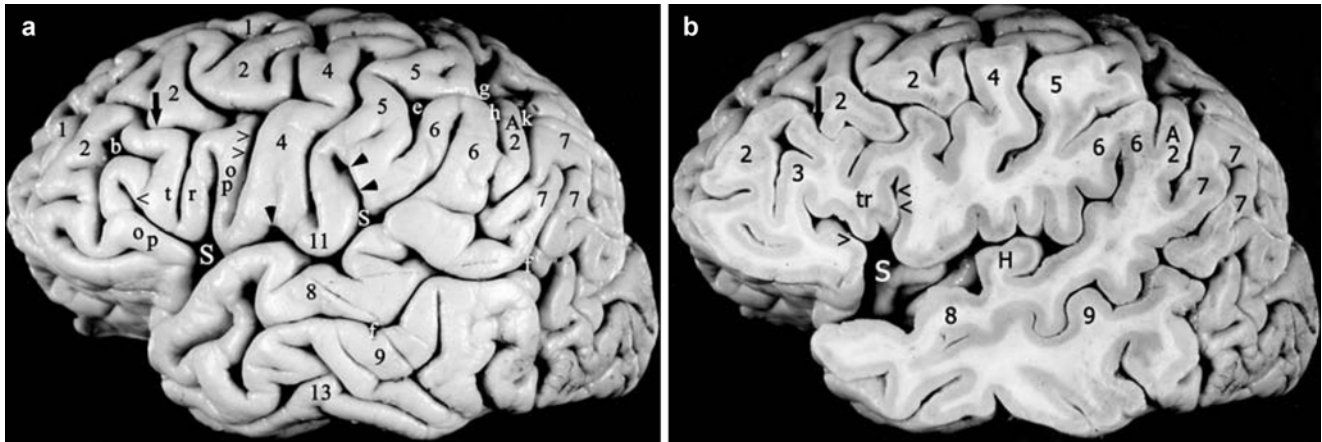
Fig. 3 (**a**, **b**) Normal variations in convexity anatomy. (**a**) Convexity surface of a prepared left hemisphere. (**b**) Sagittal section of a prepared left hemisphere. A vertically oriented connecting gyrus (*short black arrow*) crosses the inferior frontal sulcus (IFS) (*b*) to unite the pars triangularis (*tr*) with the middle frontal gyrus (MFG) (*2*). A sulcus triangularis (between the *t* and the *r*) deeply notches the superior surface of the pars triangularis making it appear bifid. The precentral gyrus (*4*) and the postcentral gyrus (*5*) unite beneath the central sulcus to form the subcentral gyrus (*11*), which is delimited by a shallow anterior subcentral sulcus (*single black arrowhead*) and a deep posterior subcentral sulcus (*double black arrowheads*). The inferior portion of the postcentral sulcus (*e*) forms the initial upswing of the arcuate intraparietal sulcus (IPS) (*g*). The posterior ascending ramus of the sylvian fissure (S)

indents the inferior parietal lobule (IPL) to form the supramarginal gyrus (SMG) (*6*). The superior temporal sulcus (STS) (*f*) indents the posterior portion of the IPL to form the angular gyrus (AG) (*7*). The entire STS parallels the sylvian fissure, hence, its synonym: parallel sulcus. The distal end of the STS within the AG may be designated the angular sulcus. In this specimen, an intercalated accessory preangular gyrus (*A2*) separates the SMG from the AG. Note the relationships of the IPS (*g*), the SMG (*6*), the AG (*7*), and the accessory preangular gyrus (*A2*) with the primary intermediate sulcus (*h*), the secondary intermediate sulcus (*j*), and the accessory intermediate sulcus (*k*). In (**b**), the sagittal section exposes the characteristic appearance of the transverse temporal gyrus of Heschl (*H*) on the superior surface of the temporal lobe (From Naidich et al. (1995); with permission)

inferior frontal gyrus (IFG) is a triangular gyrus that nestles inferiorly against the anteriormost portion of the sylvian fissure. The precentral gyrus (preCG) is a nearly vertical gyrus that forms the posterior border of the frontal lobe, behind the SFG, MFG, and IFG. The superior frontal sulcus (SFS) separates the SFG from the MFG. At its posterior end, the SFS bifurcates to form the superior precentral sulcus. The inferior frontal sulcus (IFS) separates the MFG from the IFG. At its posterior end, the IFS bifurcates to form the inferior precentral sulcus. Together, the superior and inferior portions of the preCS delimit the anterior face of the precentral gyrus, except where the MFG merges with the preCG between the superior and inferior precentral sulci.

The frontal gyri display characteristic configurations (Fig. 1) and variations (Albanese et al. 1989; Naidich et al. 1995, 1997). The IFG has an overall triangular configuration (hence, its synonym: triangular gyrus). The IFS courses above the IFG, bifurcates into the inferior preCS, and thereby separates the triangular IFG from the MFG above and from the preCG behind. The anterior horizontal and anterior ascending rami of the sylvian fissure extend upward into the triangular IFG, partially subdividing it into three portions: the *pars orbitalis*, which abuts the orbital gyri of the frontal lobe; the *pars triangularis* in the center; and the *pars opercularis*, which forms the anteriormost portion of the frontal operculum. Together, the three parts of the IFG resemble an oblique letter "M" (Figs. 1, 2, 3, and 4). Because the anterior ascending ramus of the sylvian fissure cuts through the full thickness of the IFG to reach the insula, the cortex of the
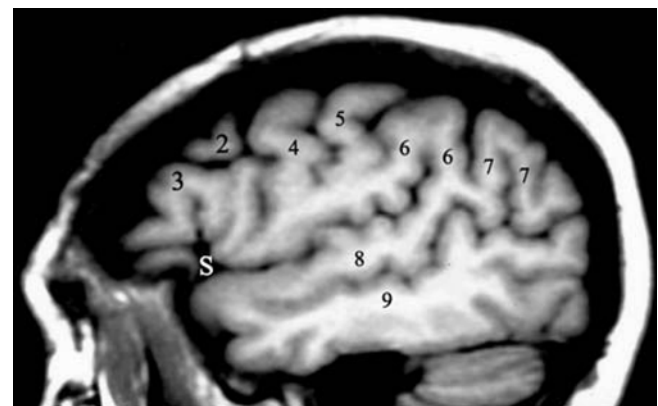

Fig. 4 Sagittal T1-weighted MR imaging of the language-related areas of the normal cerebral convexity. T1-weighted image of a 78-year-old man. Labels as in Figs. 1 and 2 (From Naidich et al. (1997); with permission)

pars opercularis presents both a superficial cortex visible on the surface and a deep cortex within the depths of the fissure (Naidich et al. 2001a).

2.1.3 Temporal Lobe

The convexity surface of the temporal lobe is formed by three horizontal gyri: the superior temporal gyrus (STG), the middle temporal gyrus (MTG), and the inferior temporal gyrus (ITG), separated by the superior temporal sulcus (STS) and the inferior temporal sulcus (ITS) (Fig. 5). The superior and middle temporal gyri extend posteriorly and then swing upward to join with the parietal lobe. The inferior temporal

Fig. 5 (**a**, **b**) The temporal lobe. Prepared anatomic specimen of the right hemisphere from a 1-day-old girl. (**a**) Convexity (reversed to match the other lateral views). The simplified gyral and sulcal pattern reflects the young age. The inferior temporal gyrus (*13*) extends posteriorly to the preoccipital notch (*large white arrowhead*). An accessory preangular gyrus (*A2*) is situated superior to the SMG (*6*) and anterior to the AG (*7*). Labels as in Figs. 1 and 2. (**b**) Inferior surface. The brainstem and the inferior thalamus have been removed to reveal the medial surface more clearly. The inferior temporal gyrus (*13*) and the inferior occipital gyrus (*19*) form the inferior margin of the hemisphere, separated by the preoccipital notch (*large white arrowhead*). The lateral occipitotemporal sulcus (*o*) delineates their medial border and separates them from the lateral occipitotemporal gyrus (LOTG) (*20*) further medially. The medial occipitotemporal sulcus (synonym: collateral sulcus) (*c*) delimits the medial border of the LOTG over its full length. Anteriorly, the collateral sulcus approximates the rhinal sulcus (*r*), and may run into it, or may parallel it. The parahippocampal gyrus (PHG) (*21*) forms the medial surface of the temporal lobe over its full length and extends posteriorly to become the isthmus (*Is*) of the cingulate gyrus inferior to the splenium (*Sp*). In the anterior half of the temporal lobe, the collateral sulcus (*c*) separates the LOTG (*20*) from the PHG (*21*). In the posterior half, the medial occipitotemporal gyrus (MOTG) (lingual gyrus) (*22*) intercalates itself between the LOTG and the PHG. The collateral sulcus stays with the medial border of the LOTG, so the collateral sulcus (*c*) separates the LOTG (*20*) from the MOTG (*22*), while the anterior calcarine sulcus (*acs*) separates the MOTG (*22*) from the PHG (*21*). The anterior and posterior transverse collateral sulci (*single and double black arrowheads*) delimit a midportion of the LOTG (*20¹*) that has been designated by Duvernoy (Duvernoy 1991) as the fusiform gyrus (From Daniels et al. (1987); with permission)
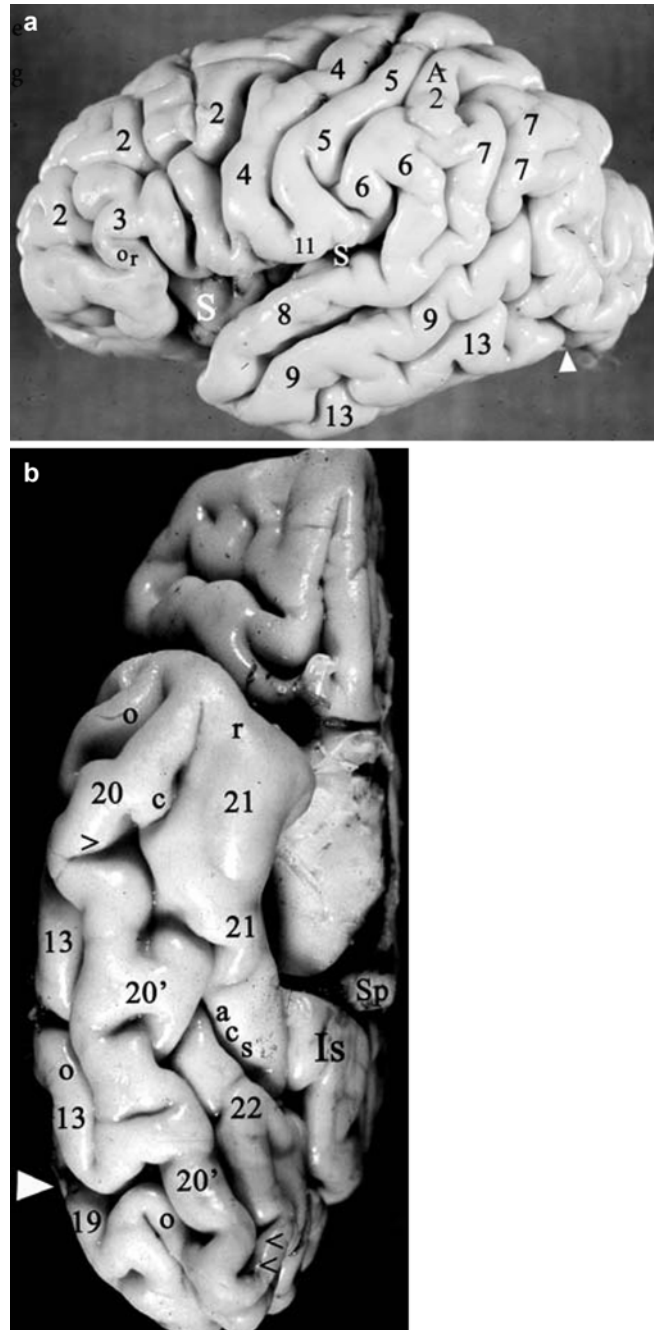
gyrus forms the inferior edge of the convexity surface of temporal lobe and curves onto the inferior surface of the temporal lobe. It is delimited posteriorly by a small notch, the preoccipital notch (synonyms: temporo-occipital notch or incisura), which separates the inferior temporal gyrus anteriorly from the inferior occipital gyrus posteriorly. The STS courses parallel to the posterior horizontal and the posterior ascending rami of the sylvian fissure (hence, its synonym, parallel sulcus). The posterior portion of the STS is directed superiorly and is sometimes designated the angular sulcus. The ITS courses approximately parallel to the inferior margin

of the convexity and may become continuous posteriorly with the inferior occipital sulcus.

2.1.4 Parietal Lobe

The convexity surface of the parietal lobe is formed by three portions: the vertically oriented postcentral gyrus (post CG) anteriorly, and the two superior parietal (SPL) and inferior parietal (IPL) lobules posteriorly (Figs. 1, 2, 3, and 4). The postCG courses vertically just posterior and parallel to the preCG. The postCG is separated from the preCG by the intervening central sulcus (CS) over most of its length.

However, inferiorly, the postCG merges with the preCG inferior to the CS along the subcentral gyrus (subCG) just above the sylvian fissure. Superiorly, the postCG merges with the preCG superior the CS along the paracentral lobule (paraCL) on the medial surface of the hemisphere. Thus, the precentral and postcentral gyri actually form a continuous band of tissue that circles around the central sulcus from the precentral gyrus through the subcentral gyrus, into the postcentral gyrus and the paracentral lobule, returning into the precentral gyrus.

The posterior border of the post CG is delimited by the superior and inferior postcentral sulci. The superior postCS separates the upper postCG from the superior parietal lobule. The inferior postCS separates the postCG from the inferior parietal lobule. The inferior postCS may be considered the upswing of a long, deep, arcuate intraparietal sulcus (IPS) that ascends behind the lower postCG and then slashes posteriorly across the convexity surface of the parietal lobe, dividing it into the SPL situated superomedial to the IPS and the IPL situated inferolateral to the IPS. The posterior downswing of the arcuate IPS then crosses the theoretical border between the parietal and occipital lobes and continues into the occipital lobe, where it is designated the intraoccipital sulcus (IOS) (synonym: superior occipital sulcus, SOS) (Figs. 1, 2, 3, and 4). Posteriorly, the SPL becomes continuous with the superior occipital gyrus (SOG) behind it through a narrow band of tissue designated the arcus parietooccipitalis (first *pli de passage* of Gratiolet) (Fig. 2) (Duvernoy 1991).

Within the inferior parietal lobule, the posterior ascending ramus of the sylvian fissure swings upward into the anterior portion of the IPL and is capped by a horseshoe-shaped gyrus designated the supramarginal gyrus (SMG). In parallel fashion, the distal STS swings upward into the posterior portion of the IPL where it is capped by a second horseshoe-shaped gyrus designated the angular gyrus (AG). The AG usually lies just posterior to the SMG, but may be displaced from that position by variant accessory gyri (Figs. 1, 2, 3, and 4) (Naidich et al. 1995, 1997). Together the SMG and the AG constitute most of the IPL. An additional small horseshoe of tissue, designated the second parieto-occipital arcus (second *pli de passage* of Gratiolet), connects the AG with the middle OG posterior to it, completing the IPL (Fig. 2) (Duvernoy 1991). A small primary intermediate sulcus descends from the IPS to separate the SMG from the AG. A small secondary intermediate sulcus descends from the IPS to define the posterior border of the AG, separating the AG from the rest of the IPL posterior to it (Naidich et al. 2001a).

2.1.5 Occipital Lobe

The convexity surface of the occipital lobe has also been divided into three horizontal gyri: the superior occipital gyrus (SOG), the middle occipital gyrus (MOG), and the inferior occipital gyrus (IOG). These are separated by the superior and inferior occipital sulci (SOS and inferior OS). The SOS (synonym: intraoccipital sulcus) is the direct continuation of the IPS (Figs. 1, 2, 3, and 4). The inferior OS is usually coextensive with the inferior temporal sulcus. Therefore, the MOG lies just posterior to the confluence of the temporal and parietal lobes at the SMG, the AG, the STG, and the MTG. The MOG is the largest portion of the occipital lobe on the convexity. It is usually subdivided into a superior and an inferior portion by a horizontally oriented middle OS (synonym: lateral OS).

2.1.6 Insula

Separating the superior and inferior covers (opercula) of the sylvian fissure discloses the Island of Reil (insula). The insula is delimited circumferentially by the peri-insular sulcus (synonym: circular sulcus), composed of the anterior, superior, and inferior perisylvian sulci (Ture et al. 1999). The central sulcus of the convexity extends over the insula as the central sulcus of the insula, dividing the insula into a larger anterior and a smaller posterior lobule (Fig. 6) (Naidich et al. 2004; Nieuwenhuys et al. 1988; Ture et al. 1999). The anterior lobule typically has three vertically oriented short insular gyri designated the anterior short, middle short, and posterior short insular gyri. These three converge anteroinferolaterally to form the apex of the insula. The posterior lobule of the insula typically displays two oblique gyri: the anterior and posterior long insular gyri. The anterior insula is connected exclusively to the frontal lobe, whereas the posterior insula is connected to both the temporal and the parietal lobes (Naidich et al. 2004; Ture et al. 1999).

2.2 Inferior Surface

2.2.1 The Frontal Lobe

The inferior (orbital) surface of the frontal lobe is formed by the gyrus rectus medially and four orbital gyri laterally, separated by the olfactory and orbital sulci. The gyrus rectus forms the medial margin of the orbital surface of frontal lobe for the full length of the frontal lobe. The lateral border of the gyrus rectus is delimited by the olfactory sulcus (Fig. 7). The orbital gyri are arranged around an "H-shaped" orbital sulcus as the medial orbital, lateral orbital, anterior orbital, and posterior orbital gyri.

2.2.2 The Temporo-occipital Lobes

The inferior surface of the temporo-occipital lobe is formed by the inferior temporal gyrus, the lateral occipitotemporal gyrus (LOTG), the medial occipitotemporal gyrus (MOTG) (synonym: lingual gyrus), and the parahippocampal gyrus (PHG), separated by the lateral occipitotemporal sulcus, the collateral sulcus, and the anterior calcarine sulcus (Fig. 5).
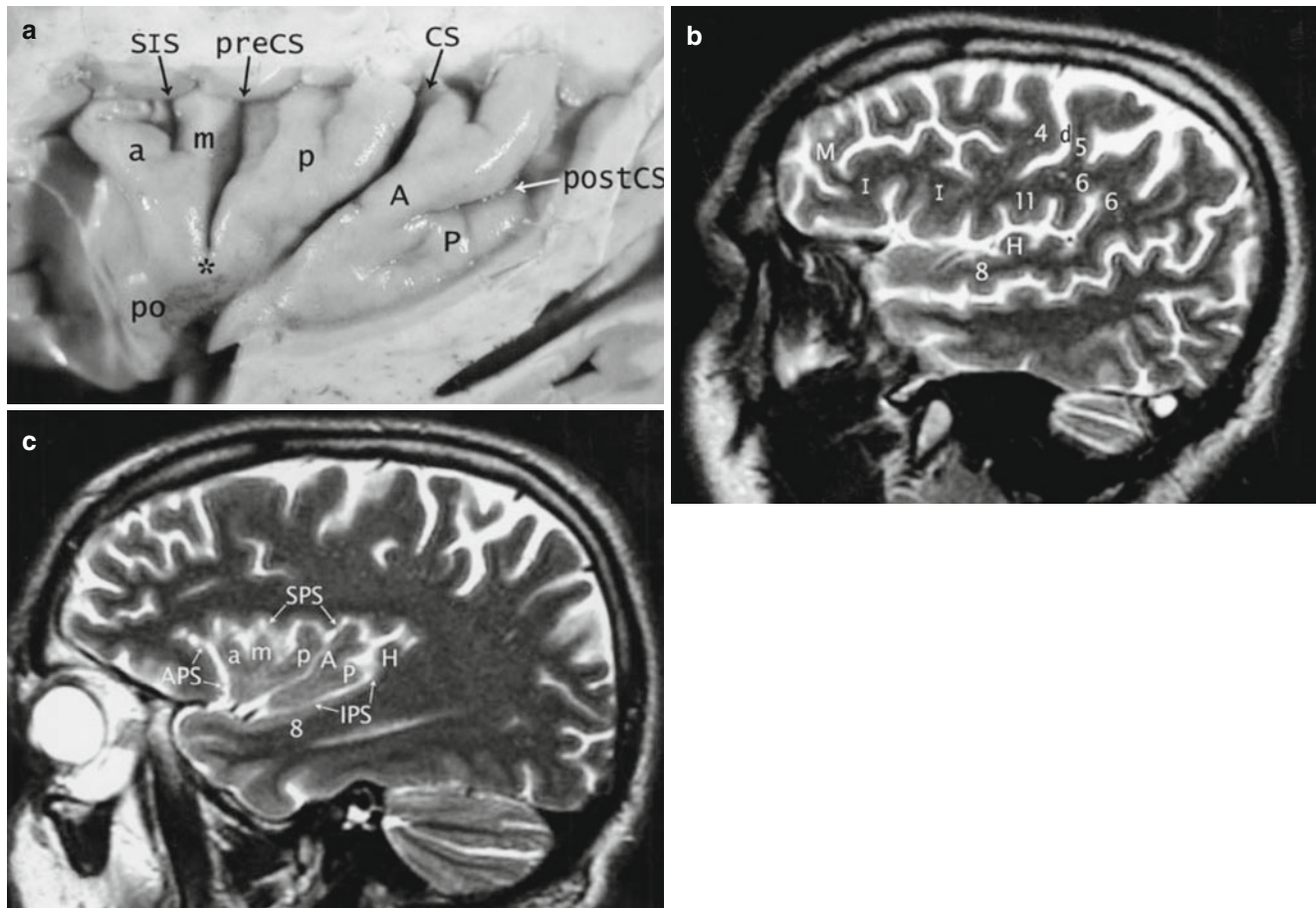
Fig. 6 (**a–c**) Insula. (**a**) Prepared anatomic specimen of the convexity surface of the insula, after removal of the overhanging opercula. A 71-year-old man. The central sulcus (*CS*) extends across the triangular insula like a "hockey stick," dividing it into a larger anterior lobule and a smaller posterior lobule. The anterior lobule typically displays three gyri, the anterior short (*a*), middle short (*m*), and posterior short (*p*) insular gyri, separated by the short insular sulcus (*SIS*) and the precentral sulcus (*preCS*). These three characteristically converge inferiorly to form the apex (***) of the insula. The posterior insular lobule typically displays two gyri, the anterior long (*A*) and the posterior long (*P*) insular gyri, separated by the postcentral sulcus (*postCS*). These too often merge together, anteriorly, just behind the central sulcus. Just inferomedial to the apex (***), the pole of the insula (*po*) forms the most anteroinferomedial portion of the insula. The central sulcus courses under the apex and the pole and then abruptly swings medially toward the supra-

sellar cistern. (**b, c**) Normal sagittal T2-weighted MRI. A 51-year-old man. Laterally (**b**), the convexity gyri form two opercula that cover the insula. Superiorly, the inferior frontal gyrus (*I*), the inferior ends of the precentral (*4*) and postcentral (*5*) gyri, the subcentral gyrus (*11*), and the supramarginal gyrus (*6*) form the frontoparietal operculum. The superior temporal gyrus (*8*) and Heschl's gyrus (*H*) form the temporal operculum. *M* middle frontal gyrus. Medially (**c**), the insula is delimited by the peri-insular sulcus, composed of three segments: the anterior (*APS*), superior (*SPS*), and inferior (*IPS*) peri-insular sulci. The anterior (*a*), middle (*m*), and posterior (*p*) short insular gyri constitute the larger anterior lobule, while the anterior (*A*) and posterior (*P*) long insular gyri form the smaller posterior lobule. The central sulcus courses between the two lobules. Heschl's gyrus (*H*) snugs up against the posteromedial portion of the posterior long insular gyrus. *8* = superior temporal gyrus (From Naidich et al. (2004) with permission)

Medially, the parahippocampal gyrus forms the medial border of the temporal lobe for the full length of the temporal lobe, from just posterior to the temporal pole to the level of the splenium. Posterior to the splenium, the medial occipitotemporal gyrus forms the medial border of the occipital lobe. Laterally, along the full length of the temporo-occipital lobes, the inferior temporal gyrus and the inferior occipital gyrus curve medially, form the inferior cerebral margin, and pass onto the inferior surface, where they constitute the lateralmost portion of the inferior surface of the temporo-occipital lobes. Only the small preoccipital

notch delimits the inferior temporal gyrus from the inferior occipital gyrus. Centrally, the LOTG runs the full length of the temporo-occipital lobes from the temporal pole to the occipital pole. Throughout its length, the LOTG remains just medial to the ITG and the IOG and is separated from them by the lateral occipitotemporal sulcus. Medially, the medial occipitotemporal sulcus (synonym: collateral sulcus) runs the full length of the LOTG (Fig. 5b). In the anterior half of the temporal lobe, the lateral occipitotemporal sulcus separates the LOTG from the parahippocampal gyrus. In the posterior half of the temporal lobe, the medial occipitotemporal
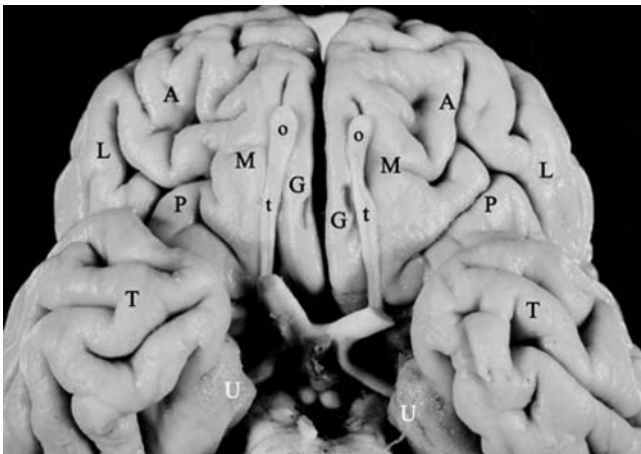
Fig. 7 Inferior surface of frontal lobe. Prepared anatomic specimen of the inferior surfaces of the anterior brain. The inferior surface of the frontal lobes is divided into two portions. The paired paramedian linear gyri recti (*G*) flank the interhemispheric fissure and are delimited laterally by the olfactory sulci, largely obscured here by the olfactory bulbs (*o*) and tracts (*t*). Lateral to the olfactory sulci, the orbital gyri of the frontal lobe are arranged around approximately H-shaped orbital sulci as the paired medial (*M*), lateral (*L*), anterior (*A*), and posterior (*P*) orbital gyri. In true base view, the anterior temporal lobes (*T*) overlap the posterior orbital gyri. Note the paired unci (*U*)

gyrus intercalates itself between the LOTG and the parahippocampal gyrus. Therefore, in the posterior half of the temporal lobe, the lateral occipitotemporal sulcus separates the LOTG form the MOTG, while the anterior calcarine sulcus separates the MOTG from the PHG.

Two synonyms are commonly used for temporo-occipital gyri. The term *lingual gyrus* usually refers to the MOTG (Duvernoy 1991; Ono et al. 1990). The term *fusiform gyrus* is most often used to designate either the LOTG (Ono et al. 1990) or a large middle portion of the LOTG that crosses the arbitrary border of the temporal and the occipital lobes between the anterior and the posterior transverse collateral sulci (Duvernoy 1991). However, in another usage, Williams et al. (1989) group the MOTG and the LOTG together as the fusiform gyrus. In most brains, the fusiform gyrus is larger on the left (Kopp et al. 1977; Naidich et al. 2001a).

2.3 Superior Surface of the Temporal Lobe

Opening the margins of the sylvian fissure, or resecting the overlying superior operculum, displays the superior surface of the temporal lobe, designated the superior temporal plane. The prominent features of this plane are one or more transverse temporal gyri (of Heschl) (Fig. 8). Heschl's gyrus or gyri (HG) arise just posteromedial to the insula and course obliquely across the superior temporal surface from posteromedial to anterolateral and may be visible at the external surface of the sylvian fissure. The presence of an HG is constant.
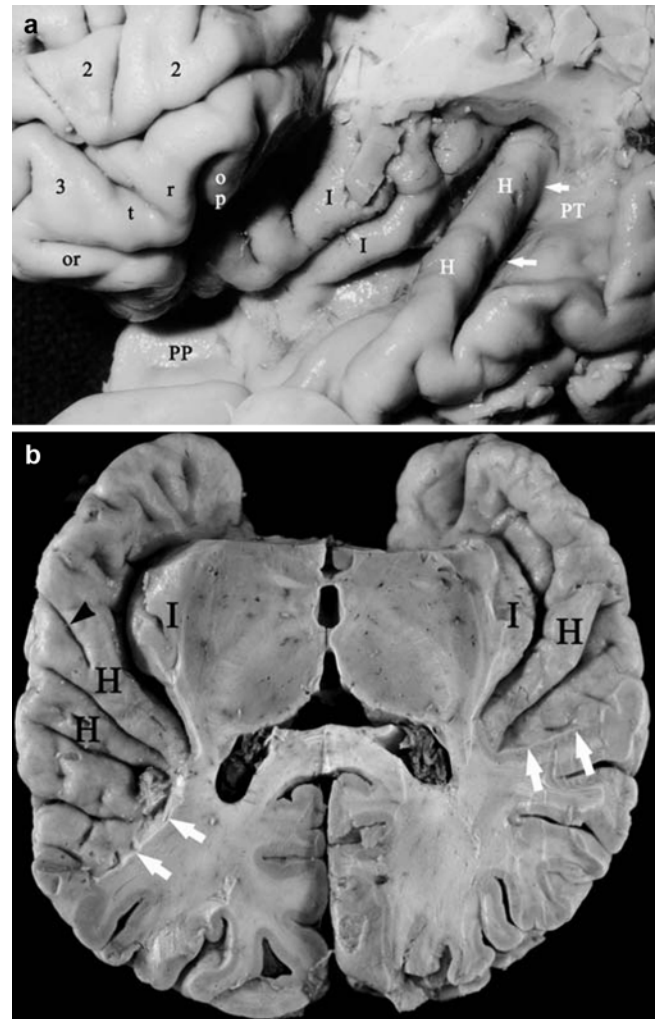

Fig. 8 (**a**, **b**). The superior surface of the temporal lobe from prepared anatomic specimens. (**a**) Anatomy of Heschl's gyrus in relation to the insula. Resection of the frontal and parietal opercula exposes the middle frontal gyrus (*2*); the pars orbitalis (*or*) triangularis (*tr*) and the residual portion of the opercularis (*op*) of the inferior frontal gyrus (*3*); the oblique long gyri (*black I*) of the posterior insula; the length of a single Heschl's gyrus (*H*) which courses obliquely across the superior surface of the temporal lobe from just posterior to the insula (posteromedially) toward the convexity surface of the superior temporal gyrus (anterolaterally); Heschl's sulcus (*white arrows*) immediately posterior to Heschl's gyrus; the planum polare (*PP*) anterior to the HG; and the planum temporale (*PT*) posterior to HG (From Naidich and Matthews (2000) with permission). (**b**) Exposure of the superior surfaces of both temporal lobes by resection of the overlying frontal and parietal opercula. Right is to the reader's right. The single right and the dual left Heschl's gyri (*H*) course obliquely across the upper surface of the temporal lobe from just posterior to the insulae (*I*) (posteromedially) to the convexity surface (anterolaterally). A shallow Beck's sulcus (*small black arrowhead*) grooves the left HG laterally. Heschl's sulcus delimits the posterior border of HG. The planum polare extends from the temporal pole to the anterior aspect of HG. The planum temporale extends between Heschl's sulcus and the posterior limit of the sylvian fissure (*white arrows*) and is substantially larger on the left

The number of HG on each side and their symmetry are highly variable. Heschl's gyri may be single (66–75 %), double (25–33 %), or triple (1 %), both unilaterally and bilaterally

(Yoshiura et al. 2000; Yousry et al. 1997a). Heschl's gyrus is often larger and longer on the left side than the right, but there is no constant relationship between HG and the side of handedness or cerebral dominance (Carpenter and Sutin 1983; Yousry et al. 1997a). A shallow longitudinal sulcus (of Beck) may groove the superior surface of HG, especially laterally, giving it a partially bifid appearance. A deep transverse temporal sulcus (Heschl's sulcus [HS]) typically defines the posterior border of HG.

The oblique Heschl's gyrus divides the superior surface of the temporal lobe into three parts. (1) The flat superior surface of the temporal lobe anterior to HG is designated the planum polare. (2) From HS at the posterior border of HG to the posterior end of the sylvian fissure, the flat superior surface of the temporal lobe is designated the planum temporale. (3) The posterosuperior extension of the planum temporale along the posterior bank of the posterior ascending ramus of the sylvian fissure may be designated the planum parietale. The planum temporale is triangular. It is typically asymmetric on the two sides and most often is larger on the left in humans, chimpanzees and other great apes (Fig. 8) (Gannon et al. 1998). The size of the planum temporale seems to correlate with the side of language dominance (and perhaps with right or left-handedness, gender, or both (Galaburda and Sanides 1980; Galaburda et al. 1998; Geschwind 1965a, b, 1970; Geschwind and Levitsky 1968; Pieniadz and Naeser 1984; Steinmetz and Seitz 1991; Steinmetz et al. 1989b, 1990a, b, 1991). Most of the variation in the sizes of the planum temporale may be ascribed to differing sizes of a cytoarchitectonic zone designated area Tpt (Galaburda and Sanides 1980). Area Tpt has a homologue in nonhuman primates that shows significant asymmetry (left > right) at the cellular level (Gannon et al. 1998).
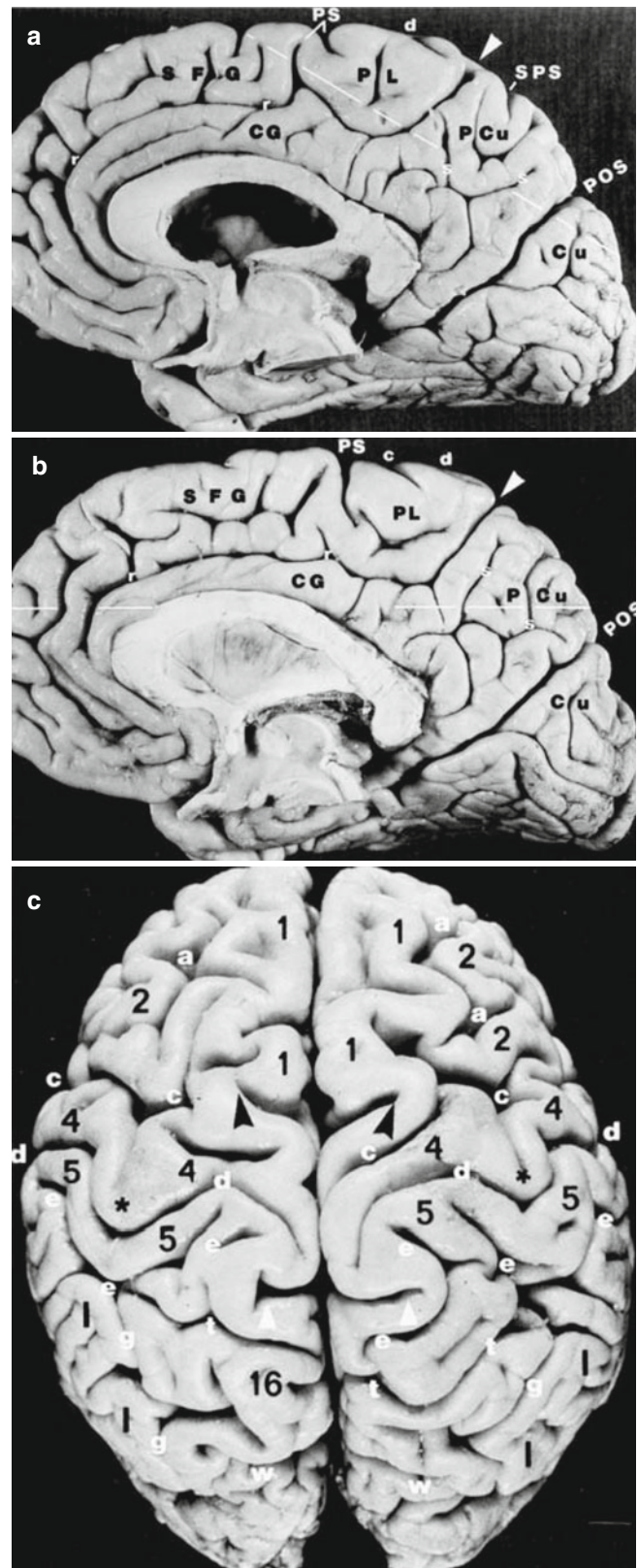
2.4   Medial Surface

The medial surface of the cerebrum is arranged as a radial array of gyri and sulci that are oriented either co-curvilinear with the corpus callosum or perpendicular to it (Fig. 9). The major gyri of the medial surface are the cingulate gyrus (CingG), the superior frontal gyrus (SFG) (whose medial surface may also be designated the medial frontal gyrus), the paracentral lobule (ParaCL), the precuneus (PreCu), the cuneus (Cu), and the medial occipitotemporal gyrus (MOTG) (synonym: lingual gyrus). The major sulci are the callosal sulcus (CalS), the cingulate sulcus (CingS), the paracentral sulcus (ParaCS), the subparietal sulcus (SubPS), the parieto-occipital sulcus (POS), the calcarine sulcus (CaS), and the anterior calcarine sulcus (AntCaS). The cingulate gyrus encircles the corpus callosum. It is delimited from the corpus callosum centrally by the callosal sulcus and from the superior frontal gyrus and paracentral lobule superficially by the cingulate sulcus.

The gyri that form the medial surface of the brain peripheral to the cingulate gyrus and sulcus are nothing more than the medial aspects of the gyri that constitute the high convexity of the brain. The superior frontal gyrus of the convexity curves over the cerebral margin onto the medial surface to form a broad arc of tissue designated the SFG or medial frontal gyrus. The precentral gyrus and the postcentral gyrus curve over the cerebral margin from the convexity onto the medial surface and join together to form the paracentral lobule. The superior parietal lobule curves over the cerebral margin onto the medial surface to form the precuneus. The superior occipital gyrus curves over the cerebral margin onto the medial surface to form the cuneus. The SFG is separated from the paracentral lobule posterior to it by the paracentral sulcus. The posterior end of the cingulate sulcus sweeps upward to reach the cerebral margin. This radially oriented distal portion of the cingulate sulcus is the pars marginalis (pM). The pars marginalis separates the paracentral lobule anteriorly from the precuneus posteriorly. The upper end of the central sulcus typically curves over the margin onto the medial surface of the hemisphere just anterior to the pars marginalis. This medial portion of the CS courses posteriorly nearly perpendicular to the pars marginalis. The "H"-shaped subparietal sulcus lies posterior to the pars marginalis and separates the inferior end of the precuneus from the cingulate gyrus deep to it. The parieto-occipital sulcus courses parallel to the pars marginalis, joins with the anterior end of the calcarine sulcus, and continues anteriorly as the anterior calcarine sulcus. The POS separates the precuneus anteriorly from the cuneus posteriorly. The calcarine sulcus separates the cuneus superiorly from the MOTG (lingual gyrus) inferiorly. The anterior calcarine sulcus separates the cingulate gyrus anteriorly from the MOTG posteriorly. The calcarine sulcus may remain entirely on the medial surface of the hemisphere, extend posteriorly to reach the occipital pole, or extend beyond medial surface onto either the convexity or inferior surfaces of the occipital lobe.

3   Lobar Borders

The precise borders of the temporal, parietal, and occipital lobes on the convexity are highly arbitrary. Published diagrams from different authors indicate substantially different criteria for partitioning the TPO lobes along the convexity (Yousry 1998). The very definitions of these borders and their lobes have evolved substantially over the years (Yousry 1998). In one common system of nomenclature, one identifies the lobes by first finding the lateral end of the deep parieto-occipital sulcus near the superior margin of the hemisphere. Then one identifies the inconstant preoccipital notch (Gusmão et al. 2002) in the inferior margin of the hemisphere (Fig. 10). The arbitrary anterior border of the occipital lobe

Fig. 9 (**a–c**) Medial and superior surfaces of both hemispheres. Prepared anatomic specimens. (**a**, **b**) Medial surfaces. The major sulci subdivide the medial surface of each cerebral hemisphere into the cingulate gyrus (*CG*), medial surface of the superior frontal gyrus (*SFG*), paracentral lobule (*PL*), precuneus (*PCu*), and cuneus (*Cu*). The posterior end of the cingulate sulcus sweeps sharply upward toward the superior cerebral margin as the marginal portion of the cingulate sulcus (pars marginalis, *white arrowhead*), which separates the paracentral lobule anteriorly from the precuneus posteriorly. Anterior to the pars marginalis, the paracentral sulcus (*PS*) arises from the cingulate sulcus and/or from the cerebral margin to separate the superior frontal gyrus from the paracentral lobule. The vertical and horizontal arms of the "H-shaped" subparietal sulcus (*s*) groove the medial surface of the precuneus and delimit it from the cingulate gyrus inferior to it. The superior ends of the vertical arms of the subparietal sulcus may reach to and notch the superior margin. The superior medial end of the central sulcus (*d*) usually crosses over the cerebral margin onto the medial surface and then recurves sharply posteriorly to course nearly perpendicular to the pars marginalis, just millimeters in front of the pars marginalis. As a consequence, the most superior medial portion of the precentral gyrus (*4*) merges with the most superior medial portion of the postcentral gyrus (*5*) around the uppermost end of the central sulcus to form the paracentral lobule anterior to the pars marginalis. A posterior portion of the postcentral gyrus passes posterior to the pars marginalis to merge with the precuneus. The prominent parieto-occipital sulcus (*POS*) courses approximately parallel to the pars marginalis, but posterior to the splenium, and delimits the parietal lobe plus cingulate gyrus anterosuperiorly from the occipital plus temporal lobes postero-inferiorly. (**c**) Superior surface of the two hemispheres. The two cerebral hemispheres border the interhemispheric fissure (*IHF*). Multiple sulci oriented at right angles to the IHF form a series of transverse grooves or "crossbars" across the IHF. The paired partes marginales (*white arrowheads*) are often the most prominent of these grooves and extend laterally into the hemispheres for a substantial distance. At the vertex, the lateral edges of the two partes marginales often curve anteriorly to form a bracket, open anteriorly. The paired central sulci (*d*) undulate across the cerebral convexity between the precentral gyri (*4*) and the postcentral gyri (*5*). They typically hook sharply posteriorly (*) as they circumscribe the hand motor region of the precentral gyrus (*), and then reverse curvature, become concave posteriorly, and converge toward the IHF just anterior to the partes marginales. The two central sulci (*d*) characteristically (but not invariably) pass anterior to and medial to the lateral edges of the partes marginales ("enter the bracket") and reach to or cross the superior margins of the hemispheres. The postcentral gyri course superiorly, behind the precentral gyri, toward or to the cerebral margins. The medial ends of the postcentral sulci (*e*) usually bifurcate around the partes marginales to form a prominent "parenthesis" configuration (*e*, *e* in the right hemisphere). The interlocking curves of the precentral gyri (*d*), postcentral gyri (*e*), and the partes marginales (*white arrowheads*) form a characteristic set of interlocking curves that usually identifies these sulci and the adjacent gyri. Other labels: (*1*) superior frontal gyrus, (*2*) middle frontal gyrus, (*4*) precentral gyrus, (*5*) postcentral gyrus, (*16*) precuneus, (*a*) superior frontal sulcus, (*c*) precentral sulcus, (*d*) central sulcus, (*e*) postcentral sulcus, (*g*) intraparietal sulcus, (*r*) cingulate sulcus, (*s*) subparietal sulcus, (*t*) superior parietal sulcus, and (*w*) parieto-occipital sulcus (From Naidich et al. (1996); with permission)
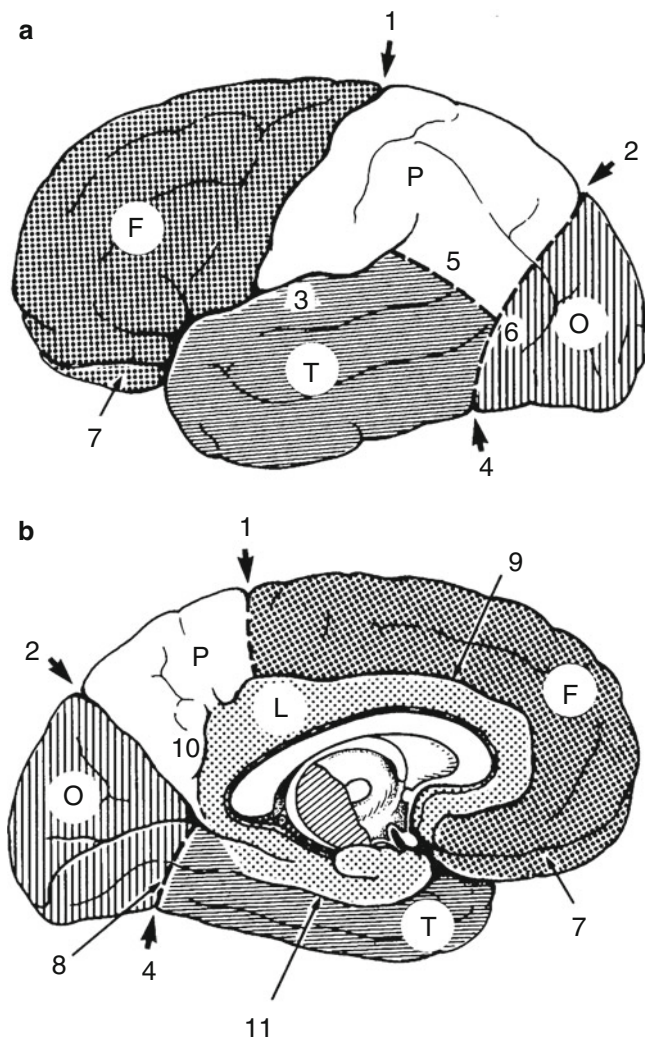
Fig. 10 (**a**, **b**) Lobar borders according to Ono, Kubik, and Abernathy. (**a**) Convexity. (**b**) Medial surface. The anterior border of the occipital lobe is delimited by the lateral parietotemporal line (*6*) drawn between the parieto-occipital sulcus and the preoccipital notch. On the convexity, the temporal lobe is separated from the parietal lobe by the temporo-occipital line (*5*) drawn from the sylvian fissure to the middle of the anterior border of the occipital lobe. On the basal surface, the temporal lobe is separated from the occipital lobe by the basal parietotemporal line (*8*) drawn from the preoccipital notch to the union of the parieto-occipital sulcus with the calcarine sulcus (unlabelled). *F* frontal lobe, *O* occipital lobe, *P* parietal lobe, *T* temporal lobe, *1* central sulcus, *2* parieto-occipital sulcus, *3* sylvian fissure, *4* preoccipital notch, *5* temporo-occipital line, *6* lateral parietotemporal line, *7* orbital surface, *8* basal parietotemporal line, *9* cingulate sulcus, *10* subparietal sulcus, *11* collateral sulcus (From Ono et al. (1990), p 9; with permission)

is then defined by the drawing the "lateral parietotemporal line" along the convexity from the lateral end of the parieto-occipital sulcus above to the preoccipital notch inferiorly.

Next one demarcates the borders of the temporal and parietal lobes that abut onto the occipital lobe. To do this, one draws the "temporo-occipital line," defined variably as (1) an

arc from the distal end of the posterior descending ramus of the sylvian fissure to the midpoint of the anterior border of the occipital lobe (Ono et al. 1990), (2) an arc from the posterior descending ramus of the sylvian fissure to the anterior border of the occipital lobe, taking care to make sure that the arc is co-curvilinear with the IPS above (Duvernoy 1991; Schwalbe 1881; Yousry 1998), (3) an arc from the posterior descending ramus of the sylvian fissure to the anterior border of the occipital lobe at the preoccipital notch (Jensen 1871; Yousry 1998), or (4) a straight linear extension from the distal end of the posterior horizontal ramus of the sylvian fissure to the anterior border of the occipital lobe (Dejerine 1895; Talairach and Tournoux 1988; Yousry 1998).

On the medial surface, the deep parieto-occipital sulcus clearly divides the parietal lobe from the occipital lobe and is the landmark used to define the anterior border of the medial occipital lobe in all systems of nomenclature. On the inferior surface, the demarcation of the lobes again becomes arbitrary. On the inferomedial surface, one may delineate the temporal lobe from the occipital lobe by drawing a basal parietotemporal line from the preoccipital notch to, variably, (1) the inferior end of the parieto-occipital sulcus where it joins the calcarine sulcus (Fig. 10) (Ono et al. 1990), (2) the anterior calcarine sulcus beneath the splenium (Fig. 11) (Duvernoy 1991), or (3) the anterior end of the anterior calcarine sulcus (Jensen 1871; Yousry 1998).

Because the patterns of sulcal branching, the gyral configurations, and the very definitions of the lobes used for anatomic description are so highly variable in this region, it may ultimately prove more accurate to designate the entire region as the TPO confluence. One could then choose to divide the convexity surface of the TPO confluence along the line of the multimodal association cortex from the lateral end of the parieto-occipital sulcus downward to, and then along, the superior temporal sulcus to define three functional compartments, a temporoparietal lobe rostral to the multimodal area (for somatosensory and auditory processing), a temporo-occipital lobe caudal to the multimodal area (for visual processing), and a TPO multimodal association lobe (for integrating the diverse modalities). On the medial surface, one could similarly use the multimodal association cortex that extends along the parieto-occipital sulcus and the anterior calcarine sulcus to divide the medial surface of the hemisphere into a medial parietal region rostral to the multimodal cortex (for somatosensory processing), a caudal temporo-occipital lobe (for visual processing), and the interposed multimodal lobe (for integration) (Naidich et al. 2001a).

The term limbic lobe signifies a broad band of tissue on the medial surfaces of the two hemispheres that, considered together, encircle the brainstem, creating a limbus about the stem. Specifically, the limbic lobe includes the subcallosal area, the cingulate gyrus, the isthmus of the cingulate gyrus, the parahippocampal gyrus, and the piriform lobe, which
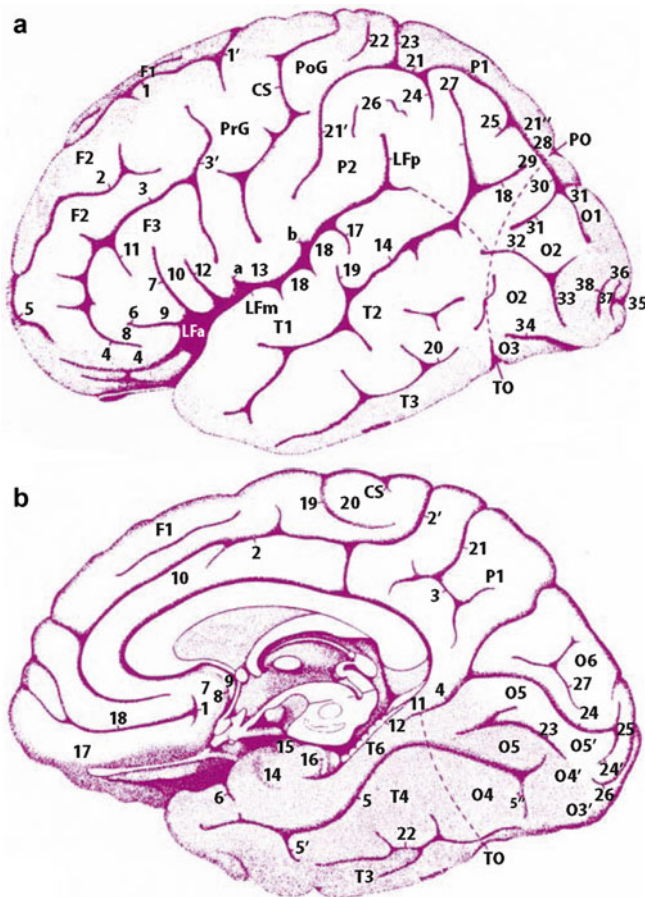
Fig. 11 (**a**, **b**) Lobar borders according to Duvernoy. (**a**) Convexity. (**b**) Inferomedial surface. The anterior border of the occipital lobe is delimited by the same lateral parietotemporal line drawn between the parieto-occipital sulcus and the preoccipital notch. On the convexity, the temporal lobe is separated from the parietal lobe by a temporo-occipital line drawn co-curvilinear with the intraparietal sulcus from the posterior descending ramus of the sylvian fissure to the anterior border of the occipital lobe. On the basal surface, the temporal lobe is separated from the occipital lobe by a basal parietotemporal line drawn from the preoccipital notch to the anterior calcarine sulcus inferior to the splenium. The posterior end of the superior temporal sulcus bifurcates as it extends into the inferior parietal lobule, making a large angular gyrus (a common variation). The fusiform gyrus is formed from portions of the temporal lobe (*T4*) and the occipital lobe (*O4*) that occupy the midportion of the lateral occipitotemporal gyrus between the anterior (*5′*) and posterior (*5″*) transverse collateral sulci. Convexity surface (**a**) *LFa*, *LFm*, and *LFp* = lateral fissure (anterior, middle, and posterior segments); *CS* central sulcus, *PO* parieto-occipital fissure, *TO* =temporo-occipital incisure, *F1*, *F2*, and *F3* = superior, middle, and inferior frontal gyri; *PrG* precentral gyrus, *T1*, *T2*, and *T3* = superior, middle, and inferior temporal gyri; *P1* = superior parietal gyrus (lobule); *P2* = inferior parietal gyrus (lobule); *PoG* postcentral gyrus, *O1*, *O2*, and *O3* = superior, middle (synonym: lateral), and inferior occipital gyri; *21*, *21′*, and *21″* = intraparietal sulcus; *33* = sulcus lunatus. Inferomedial surface (**b**) *P1* precuneus, *T3* inferior temporal gyrus, *T4* temporal portion of the fusiform gyrus, *T5* parahippocampal gyrus, *TO* temporo-occipital incisure, *O3* inferior occipital gyrus, *O4* occipital portion of the fusiform gyrus, *O5* lingual gyrus, *O6* cuneus, *2* cingulate sulcus, *2′* marginal segment of the cingulate sulcus (pars marginalis), *3* subparietal sulcus, *4* anterior calcarine sulcus, *22* lateral occipitotemporal sulcus, *24* calcarine sulcus. The caudal portions of *O3*, *O4*, and *O5* merge together at the inferior aspect of the occipital lobe (From Duvernoy (1991), pp 5–9; with permission)

according to Duvernoy corresponds to the anterior parahippocampal gyrus (Duvernoy 1991).

Recently, Yasargil emphasized the arbitrary and uncertain borders between the lobes and proposed a new lobar classification in which the continuous circle of tissue formed by the precentral gyrus, subcentral gyrus, postcentral gyrus, and paracentral gyrus was considered to be a separate, distinct *central* lobe. Thus, the Yasargil classification would include seven lobes, the frontal central, parietal, occipital, temporal, insular, and limbic lobes (Yasargil 1994).

4 Localizing Anatomic Sites Independent of Lobar Anatomy

Several attempts have been made to identify functionally relevant anatomic sites, *independent of* the variable lobar and sulcal borders. These systems depend on first establishing reference planes that are based upon a very limited number of deep anatomic structures, then designating all locations in space in terms of coordinates based upon those limited reference planes, and finally identifying all other anatomic features in terms of these coordinates. These attempts may be extended to "correct for" differences in overall head and brain shape by "morphing" the anatomy of any individual brain to superimpose its gross contours on those of a single standard anatomic reference brain. Applied to groups of patients, such systems may detect commonalities otherwise obscured by individual variation, but at the costs of (1) information specific to each individual and (2) understanding of the range of normal variation.

4.1 Talairach-Tournoux Coordinate System and "Talairach Space"

Talairach and Tournoux took a horizontal plane that extended through the brain along a line drawn from the top of the anterior commissure (AC) to the bottom of the posterior commissure (PC). The line is the AC-PC line. The horizontal plane through the anterior and posterior commissures is the Talairach-Tournoux baseline. From this baseline, a vertical plane is raised perpendicular to the baseline at the top of the anterior commissure. This is the VAC (vertical at the anterior commissure). A second similar vertical plane is raised perpendicular to the baseline at the bottom of the posterior commissure. This is the VPC (vertical at the posterior commissure). These planes define the coronal position. The third orthogonal plane is taken as the midline vertical plane through the AC-PC line. All anatomic positions are then defined by their coordinates in the vertical direction (designated from superior to inferior as 1–12), anteroposterior direction (A to I), and transverse direction (designated from

the midline to lateral as a–d). Thus, the central sulcus is found in "a,1–2, F" of the left or right hemisphere. These coordinates are considered to exist in "Talairach space" independent of any sulcal or lobar borders.

5　Identification of Specific Anatomic Structures

5.1　The Pericentral Cortex

The pericentral region consists of two parallel gyri, the precentral and postcentral gyri, separated by the CS. Superiorly, the CS nearly always reaches the cerebral margin and may extend onto the medial interhemispheric surface of the brain. In this location, the precentral and postcentral gyri fuse to each other to form the paracentral lobule around the upper end of the CS. Inferiorly, the CS rarely reaches the sylvian fissure. Instead, the preCG and postCG fuse together to form the subcentral gyrus between the inferior end of the CS and the sylvian fissure. This is partially delimited anteriorly and posteriorly by the anterior and posterior subcentral sulci (Fig. 9). Functional and anatomical MRI have both been used to define significant regions along the preCG (primary motor cortex) and the postCG (primary sensory cortex).

5.1.1　Functional Methods

Functional MRI (fMRI) shows that the motor hand area is located at the middle genu of the CS in a portion of the preCG that displays a characteristic omega or epsilon-shaped "knob" or "knuckle" (Naidich and Brightbill 1996b; Yousry et al. 1997b). Using MEG (magnetoencephalography), it is possible to identify the postCG reliably (Sobel et al. 1993). Using PET (positron emission tomography), it can be shown that the cortical representation of the sensory hand area is located along the anterior bank of the postCG at a characteristic curve of the CS immediately posterior to the motor hand area (Rumeau et al. 1994). On fMRI, detection of an "activated" vein can assist in the identification of the CS, especially in patients with tumors distorting the cortical anatomy (Yousry et al. 1996). Currently fMRI is increasingly used to define the central region preoperatively.

5.1.2　Anatomical Methods

CT has shown that the marked normal variability of the cortical anatomy can limit the use of standard systems for localizing anatomy, such as the Talairach space (Steinmetz et al. 1989a). Therefore, specific signs have been developed to help to identify the individual portions of the pericentral region more directly (Iwasaki et al. 1991; Naidich and Brightbill 1995, 1996a, b; Naidich et al. 1995; Yousry et al.
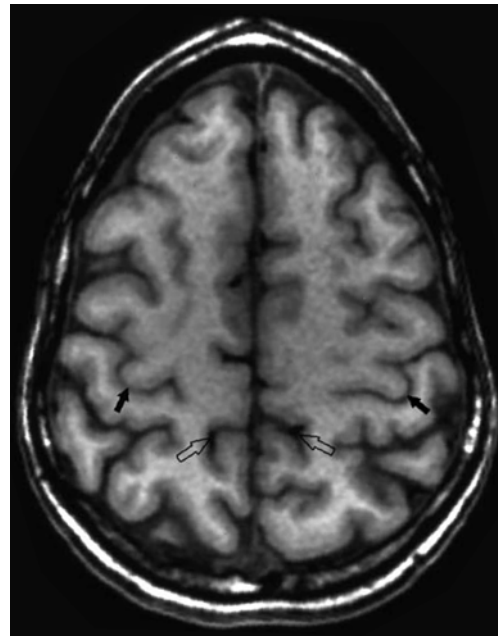

Fig. 12 Pericentral region. Axial landmarks. In the axial plane (T1-weighted MPRAGE sequence), the Ω-shaped knob of the precentral gyrus is easily identified (*arrows*). The pars marginalis of the cingulate sulcus of both hemispheres appears as a horizontal bracket (*open arrows*). The medial end of the central sulcus enters the pars bracket immediately anterior to the pars. The full sagittal dimension of the precentral gyrus is thicker than that of the postcentral gyrus. The cortex of the precentral gyrus is thicker than the cortex of the postcentral gyrus

1995, 1997b). The sensitivity and specificity of these signs have been evaluated and the multiple signs combined into a system for localizing the CS and related gyri (Naidich and Brightbill 1996b). Three axial and three sagittal signs are most important. These signs should always be used together, systematically, so that the failure of any one sign is corrected by the concordance of localization given by the other signs (Naidich and Brightbill 1996b).

- Axial Plane Images

The precentral knob: a focal, posteriorly directed protrusion of the posterior surface of the preCG, designated the precentral knob, has been shown by fMRI to be the site of the hand motor area. This focal motor region is seen on axial CT and MRI images as an inverted omega (90 %) or as a horizontal epsilon (10 %) in all cases (Fig. 12). This sign has a high inter-rater reproducibility (Yousry et al. 1997b) as well as high "applicability (Naidich and Brightbill 1996b).

The pars bracket sign: in axial plane CT and MRI, the pars marginalis of the cingulate sulcus of the left and the right cerebral hemispheres appear together as a horizontal bracket. The medial end of the CS enters the pars bracket immediately anterior to the pars marginalis in 94–96 % of cases (Fig. 12), whereas the postcentral sulcus enters

the pars bracket in only 3 %. Thus, the relationship of a sulcus to the pars bracket permits accurate identification of the CS (the "bracket sign"). This sign is also characterized by a high applicability (Naidich and Brightbill 1996a, b).

Thickness of the pre- and postcentral gyri: the full sagittal dimension of the preCG is thicker than that of the postCG (Fig. 12) (Naidich and Brightbill 1996b; Naidich et al. 1995). Further, the posterior *cortex* of the preCG is also thicker than the anterior cortex of the postCG at the corresponding site on the other side of the central sulcus (Meyer et al. 1996). Using T1-weighted turbo inversion recovery sequences, the mean cortical thicknesses of the anterior (preCG) and posterior (postCG) banks of the CS were found to be 2.70 and 1.76 mm for both hemispheres with a mean cortical thickness ratio of 1.54 (Fig. 12) (Meyer et al. 1996). The difference in cortical thickness is based on and explained by cytoarchitectonic studies (Brodmann 1909; Naidich and Brightbill 1996b; von Economo and Koskinas 1925). These three signs are the most important and most reliable for attempting to localize the CS in the axial plane (Naidich and Brightbill 1996b).

• Sagittal Plane Images

Lateral sagittal plane. The "M" shape of the inferior frontal gyrus. The anterior horizontal and anterior ascending rami of the sylvian fissure extend upward into the IFG, giving it the shape of a letter "M." The first vertical line of the "M" represents the pars orbitalis. The middle "v" of the "M" represents the pars triangularis. The posterior vertical line of the "M" represents the pars opercularis of the IFG. Identification of the "M" provides the starting point for subsequent, sequential identification of the preCS, preCG, CS, and postCG (Fig. 13) (Naidich et al. 1995, 1997; Steinmetz et al. 1990a).

Middle sagittal plane: the precentral knob. The posteriorly directed expansion of the preCG at the hand motor area may be identified at the level of the insula as a posteriorly directed hook, which fits neatly into the concavity of the hand sensory region of the postcentral gyrus. This configuration defines the position of the preCG, the CS, and the postCG in 92 % of cases (Fig. 13) (Yousry et al. 1997b).

Medial sagittal plane: the pars marginalis. The posterior portion of the cingulate sulcus, which sweeps upward to reach the cerebral margin, is the pars marginalis. The CS lies millimeters anterior to the pars marginalis. Characteristically the portion of the CS that lies on the medial surface of the brain curves posteriorly to course nearly perpendicular to the pars marginalis (Fig. 13) (Naidich and Brightbill 1996b).

5.2 The Superior Temporal Plane

The transverse temporal gyrus of Heschl courses anterolaterally over the superior surface of the temporal lobe from the posterior border of the insula medially to the convexity surface of the temporal lobe laterally. HG corresponds to Brodmann's area 41 (Brodmann 1909), the primary auditory cortex (A1). Usually, only a restricted posteromedial portion of HG can be considered the true site of A1 (Liegeois-Chauvel et al. 1991). A second HG may be present posterior and parallel to the first and may occasionally be functionally included in A1 (Liegeois-Chauvel et al. 1995).

Using MRI, HG may be identified accurately in the axial, sagittal, and coronal planes. In the *sagittal plane*, HG has a characteristic shape easily identified on the supratemporal surface just lateral to the insula. Depending on the number of HG present, HG may assume the form of a single "omega," a "mushroom," a "heart," or a double Ω (Fig. 14) (Yousry et al. 1997a). In the *coronal plane* perpendicular to the Talairach-Tournoux baseline, HG is found best in the section that displays the (tentlike) convergence of the two fornics and the eighth cranial nerves (Fig. 14) (Yousry et al. 1997a). In the *axial plane*, HG is found most easily in the section which displays the massa intermedia of the thalamus (Fig. 14) (Yousry et al. 1997a).

5.3 The Occipital Lobe

The occipital lobe is important for the visual areas (V1–V3, Brodmann's areas 17–19) it contains. The primary visual area (V1, Brodmann's area 17) is located in the striate cortex. Most of the striate cortex extends along the calcarine sulcus (Korogi et al. 1996). However, the precise site of the striate cortex is variable. The striate cortex may be exposed on the medial surface of the occipital lobe, lie hidden within the depths of the calcarine sulcus, extend into the parieto-occipital or anterior calcarine sulci, and/or lie on the tentorial surface of the occipital lobe (Korogi et al. 1996). The precise configuration of the calcarine sulcus also varies (Fig. 15). Korogi et al. found that the sulcus could be a single continuous sulcus without major branches (50 %), could give off major branches (26 %), and could even show significant disruptions (24 %) (Korogi et al. 1996). In the coronal plane, the calcarine sulci and parieto-occipital sulci were symmetric in only 60 % of cases. One calcarine sulcus was significantly lower than the other in 24 % (by more than 10 mm in 12 % of cases (Korogi et al. 1996). The calcarine and the parieto-occipital sulci formed a "V" in 16 % (Korogi et al. 1996). The exact positions and (a) symmetries of the calcarine and parieto-occipital sulci are also influenced by the magnitude of any occipital petalia. These variations complicate the identification of the calcarine sulcus (Yousry et al. 2001).
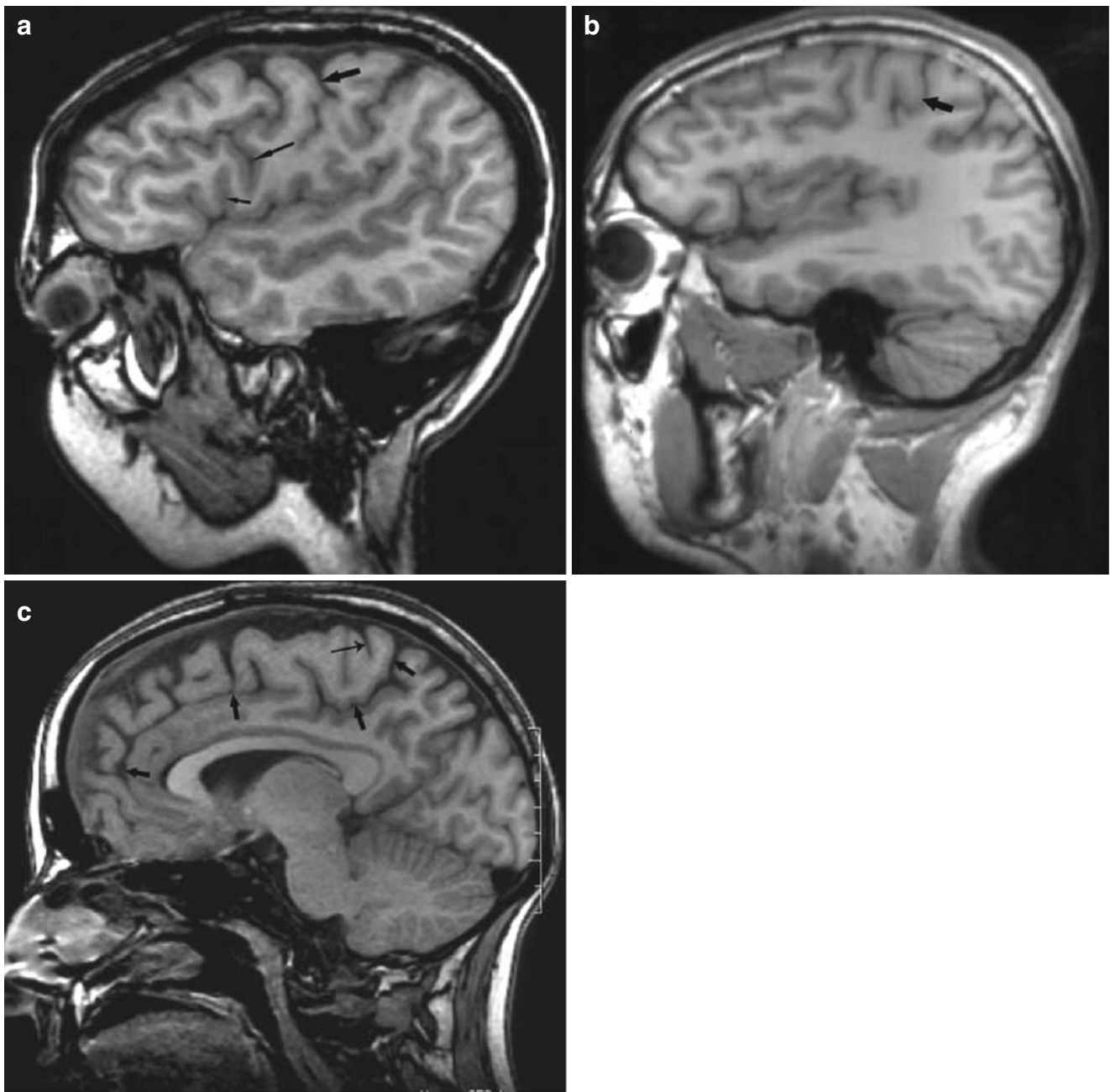
Fig. 13 (**a**–**c**) Pericentral region. Sagittal landmarks (T1-weighted MPRAGE sequence). (**a**) In the sagittal plane, the anterior horizontal ramus (unlabeled anteriorly) and anterior ascending ramus (*short thin arrow more posteriorly*) of the sylvian fissure are first identified on the lateral sections and used to identify the M shape of the inferior frontal gyrus. Posterior to this gyrus, in order, lie the precentral gyrus (*long thin arrow*), the subcallosal gurus, the central sulcus (*short thick arrow*), and the postcentral gyrus. (**b**) At the level of the insula, the posteriorly directed hook (*arrow*) of the motor hand area defines the precentral gyrus. (**c**) The cingulate sulcus and its ramus marginalis (*arrows*) are first identified. The central sulcus (*thin arrow*) lies immediately anterior to the pars marginalis and is oriented such that it curves posteriorly, to course nearly perpendicular to the ramus marginalis

6 Cortical Architecture

6.1 Cytoarchitectonics

The neocortex exhibits six cell layers characterized by differing proportions of cell types, cell densities, and myelination of fibers. From superficial to deep, the six neocortical layers are designated by Roman numerals: (I) molecular layer, (II) external granule cell layer, (III) external pyramidal cell layer, (IV) internal granule cell layer, (V) internal pyramidal cell layer, and (VI) multiform layer. Further variations within each layer may lead to subdivisions such as layers IVA and
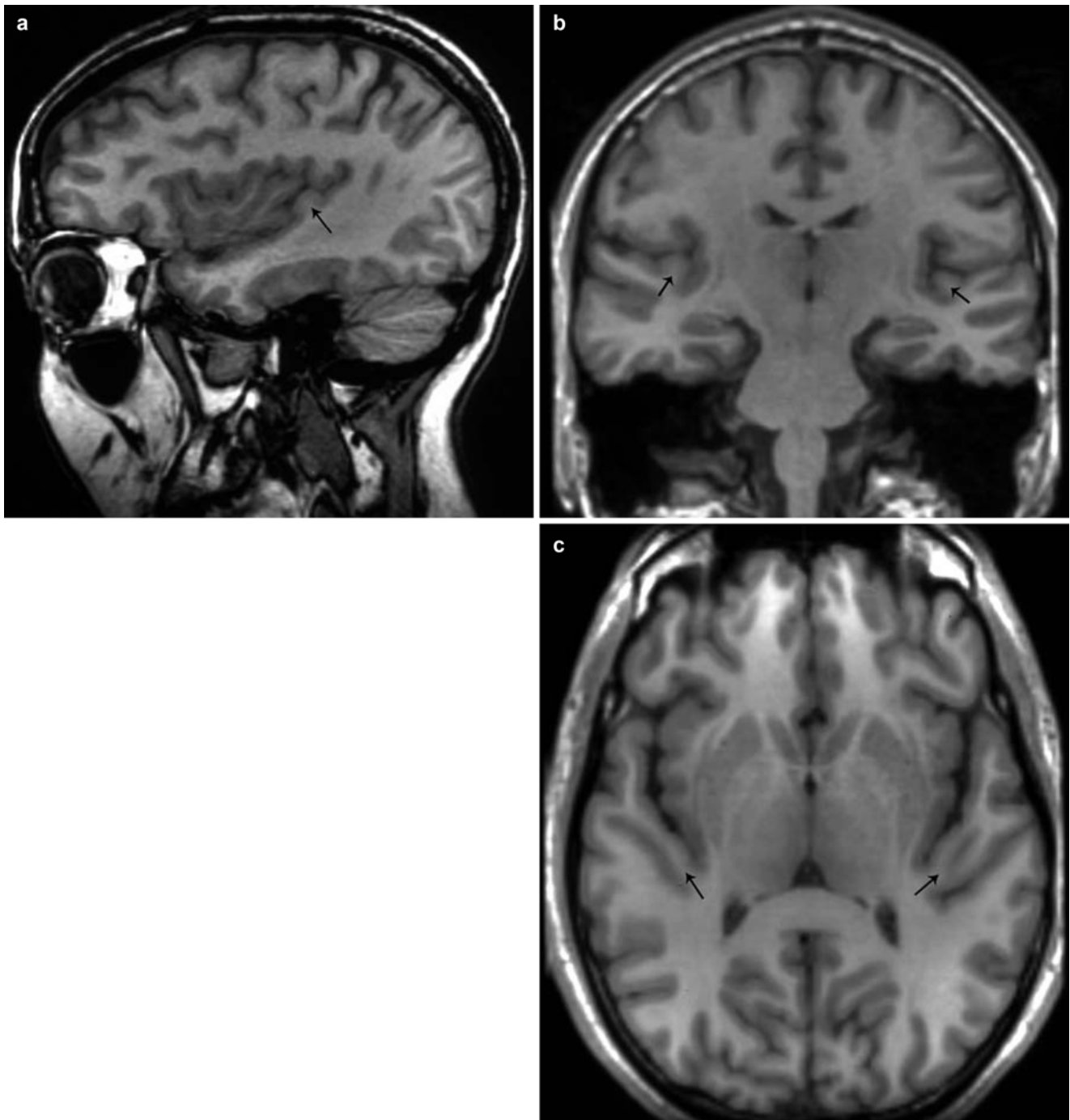
Fig. 14 (**a**–**c**) Heschl's gyrus. Landmarks in three planes (T1-weighted MPRAGE sequence). (**a**) In the sagittal plane just lateral to the insula, the shape of HG (*arrow*) is so characteristic that it can easily be identified directly on the supratemporal surface without the need for additional landmarks. Depending on the presence and extent of any intermediate sulcus, HG may appear Ω-shaped, on medial sections of the temporal lobe and insula. (**b**) In a coronal plane perpendicular to the bicommissural plane, the section on which HG (*arrows*) is identified best is characterized by (*1*) a tentlike shape formed as the two fornices converge to join with each other and (*2*) the presence of the eighth cranial nerves. (**c**) In the axial plane, HG (*arrows*) is identified by its temporal location and its characteristic anterolateral course on the section in which the adhesion interthalamica (massa intermedia) can be identified

IVB. In general, afferent fibers to the cortex synapse in layers I–IV. Afferents from specific thalamic nuclei end predominantly in layer IV. Efferents from the cortex arise in layers V and VI. Those efferents directed to the brainstem and spinal cord arise mainly in layer V (Carpenter and Sutin 1983; Gilman and Newman 1996).
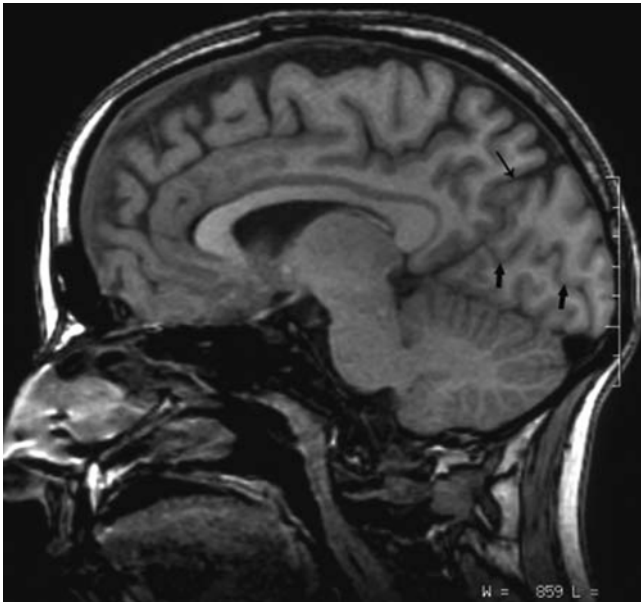
Fig. 15 Occipital lobe (T1-weighted MPRAGE sequence). The calcarine sulcus (*arrows*) runs obliquely in an anterosuperior direction from the occipital pole to its junction with the parieto-occipital sulcus (*thin arrow*) to form the anterior calcarine sulcus. The calcarine sulci show a gradual posterior declination

Fig. 16 (**a**, **b**) The five types of cerebral isocortex are distributed over the convexity (**a**) and medial surface (**b**) of the cerebral hemisphere. Cortex type *1* agranular (motor) heterotypical, *2* frontal homotypical, *3* parietal homotypical, *4* polar homotypical, *5* granulous (sensory) heterotypical (koniocortex). Note that the words frontal and parietal used in this way signify types of isocortex and not anatomic locations or lobes (From von Economo and Koskinas (1925); with permission)

Granule cells are small polymorphic (stellate, tufted, or bipolar) cells that form the major component of the external and internal granule cell layers (II and IV). These are mainly γ-aminobutyric acid-(GABA)-ergic inhibitory neurons. Pyramidal cells are pyramid-shaped cells with their apical dendrites directed superficially to layer I. The basal dendrites span outward laterally. The major axon arises from the base of each pyramidal cell to pass to its target. Small pyramidal cells found in layers II, III, and IV project to intracortical regions (Gilman and Newman 1996). Large pyramidal cells in layer V project to the brainstem and the spinal cord (Gilman and Newman 1996). Giant pyramidal cells with direct corticomotoneuronal connections to the (alpha) motoneurons of the brainstem and the spinal cord are designated Betz cells. In humans, Betz cells are found exclusively in the primary motor cortex (M1).

Throughout the cortex, the cell layers differ in their total thickness, the thickness of each layer, the concentrations of cells within each layer, the conspicuity of each layer, the degree of myelination of the fibers within the layer, and the presence or absence of special cells, like the Betz cells. These variations give each region a specific cytoarchitecture that subserves the function of that region. The cytoarchitectonic variations in the cortex lead to classifications of cortical regions by their cytoarchitecture. If the six-layered neocortical organization is readily discernable, the cortex is designated homotypical. If focal specialization of the cytoarchitecture partly obscures these layers, the cortex is
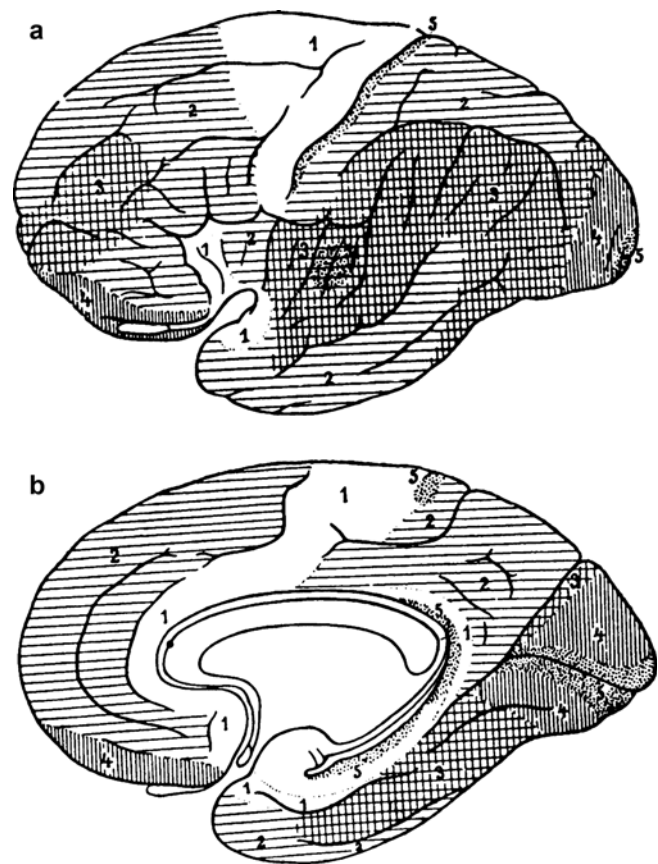
designated heterotypical (von Economo and Koskinas 1925). von Economo and Koskinas (1925) grouped the cortical regions into five types (Fig. 16). Three types were considered homotypical: frontal cortex, parietal cortex, and polar cortex. Two were considered heterotypical cortices: the agranular cortex (specialized for motor function) and the koniocortex (specialized for sensory function). Brodmann (1909) recognized additional variations in cortical architecture, subdivided the cortex into approximately 40 distinct cytoarchitectonic areas, and tried to relate the cortical architecture to function. These regions are now designated the Brodmann's areas (BA) (Fig. 17).

In humans, the motor cortex is formed of three major cortical types:

- The heterotypical agranular isocortex is characterized by increased overall thickness, significantly reduced to absent granule cells in layer IV, and thick well-developed layers of large pyramidal cells in layers III and V (Zilles et al. 1996). In this agranular cortex, even the small cells
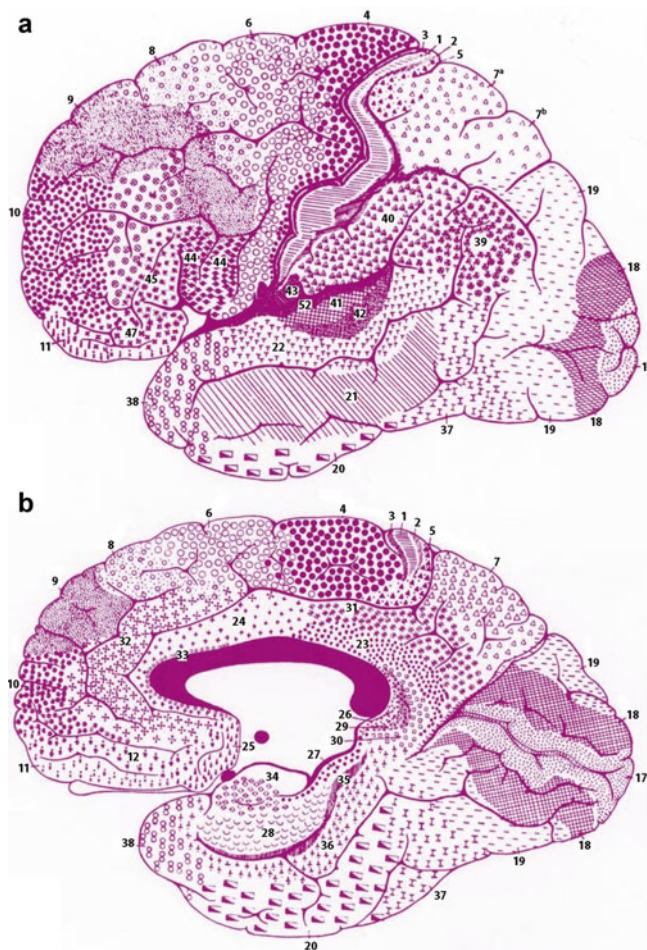
Fig. 17 (**a**, **b**) Cytoarchitecture of the human cortex. Convexity (**a**) and medial (**b**) surface views of Brodmann's areas. Symbols indicate Brodmann's parcellation of the cortex into the cytoarchitectonic areas that are designated by the Brodmann's area (BA) numbers assigned. Compare with Fig. 1 (Parts **a**, **b** *from* Carpenter and Sutin (1983); with permission)

Fig. 18 Somatotopy of the primary motor cortex (M1): the motor homunculus, as described by Penfield and Jasper (From Williams et al. (1989); with permission)

in layers II (and the region of IV) are predominantly pyramidal in shape. Type (a) corresponds predominantly to BA 4, 6, 8, 24, 44, and 45 and is found in the posterior half of the precentral gyrus, the anterior half of the cingulate gyrus, the anterior portion of the insula, and in a narrow strip which extends from the retrosplenial portion of the cingulate gyrus into the parahippocampal gyrus (Figs. 16 and 17). Within these areas, the primary motor cortex, designated M1 (Brodmann's area 4), is characterized by the presence of giant Betz cells in lower layer V (Zilles et al. 1996). The motor speech areas, BA 44 and BA 45, are found in the inferior frontal gyrus.

- The homotypical frontal cortex is characterized by narrow granule cell layers composed of loosely arrayed small granule cells and by prominent small- and medium-sized pyramidal cells in layers III and V (Carpenter and Sutin 1983). Giant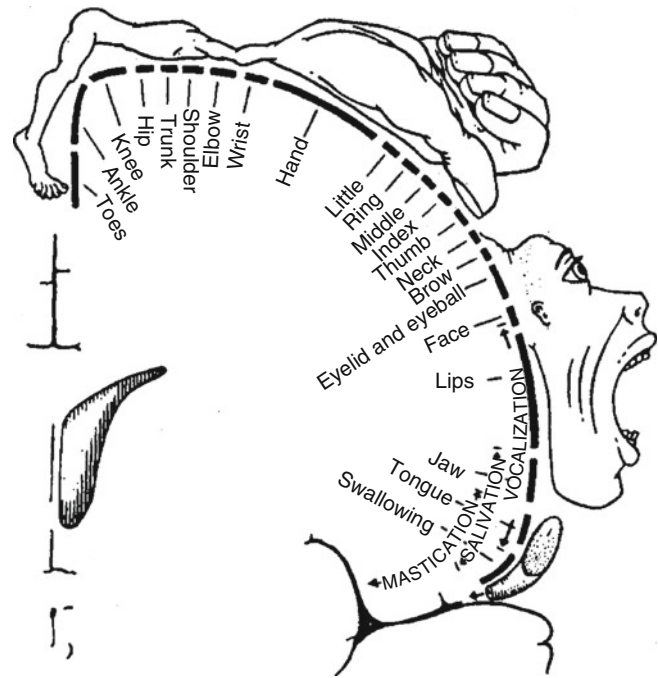 Betz cells are absent. This frontal cortex corresponds to BA 9, 10, 11, 46, and 47 and is found along the convexity and the anteriormost medial surfaces of the superior and middle frontal gyri.

- The homotypical polar cortex is characterized by overall cortical thinness, well-developed granule cell layers, and a comparative wealth of cells (Carpenter and Sutin 1983; Naidich et al. 2001b). It corresponds to BA 10.

6.2 Somatotopy

The term somatotopy refers to the topographic organization of function along the cortex. It is a map of the sites at which smaller or larger regions of cortex form functional units that correspond to body parts or to motions across a joint. In specific regions like the primary auditory cortex, the somatotopy may be described by a more specific word such as tonototopy. For white matter, the preferred term is myelototopy. The presence of somatotopy signifies that the functional activity of the cortex is organized topographically along the cortex. Absence of somatotopy signifies that medicine has failed, thus far, to appreciate any topographic organization of that cortex. Somatotopy may be fine, as in the primary motor cortex (BA 4), where relatively restricted zones of cortex correspond to defined manipulation units (Fig. 18). It may be very fine, as in the hand motor area along the precentral gyrus, where there may be representation for the motion of each individual digit. Alternatively, somatotopy may be very
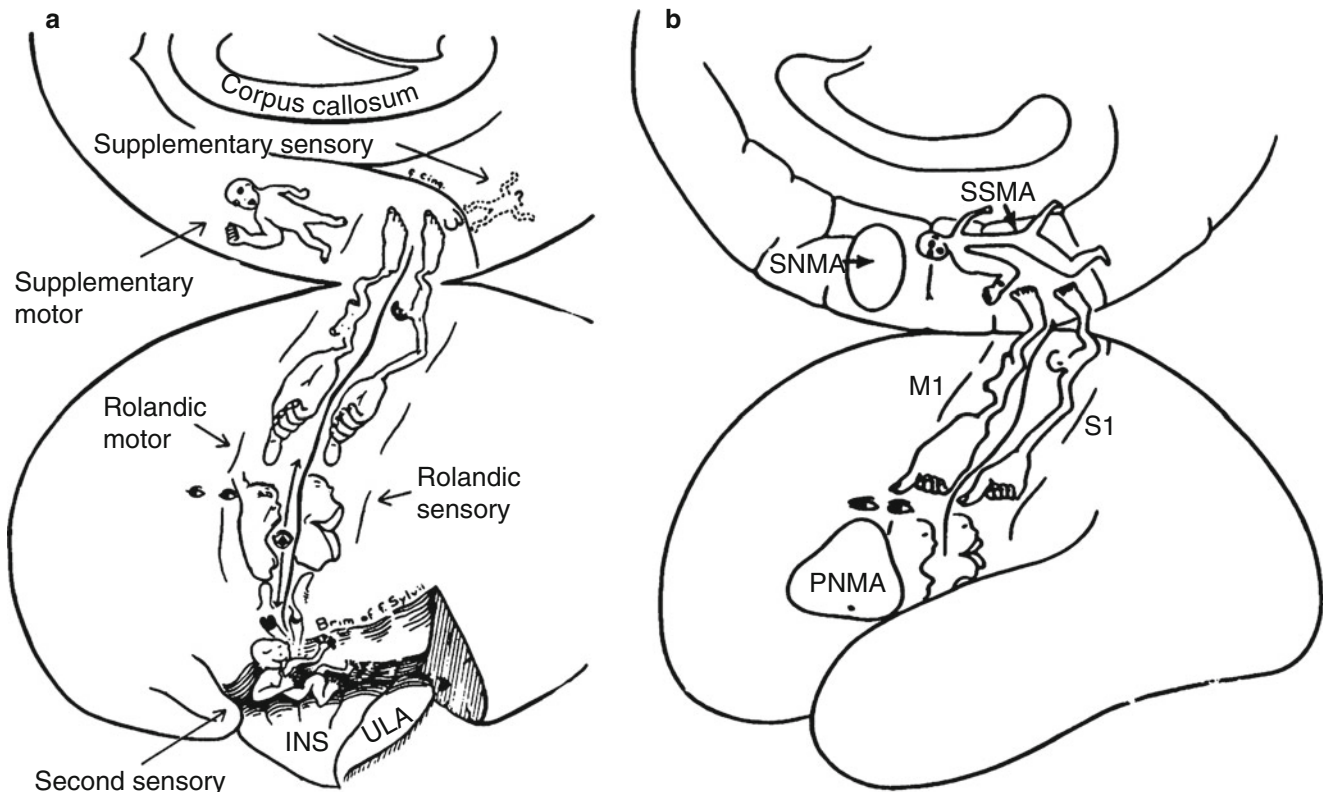
Fig. 19 (**a**) Somatotopy of the supplementary motor areas (*SMA*) as represented by Penfield and Jasper. (**b**) Somatotopy of the pre-SMA (the supplementary negative motor area [*SNMA*]) and the relation of the pre-SMA to the SMA, simplified from Penfield and Jasper. *M1* primary motor cortex, *PNMA* primary negative motor cortex, *S1* primary sensory cortex, *SSMA* supplementary somatosentory cortex (**a** From Luders (1996); (**b**) From Freund (1996); with permission)

crude, as in the SMA, the pre-SMA, and the cingulate motor cortex (CMC), where cortical zones seem to correspond to broad regions, such as head, trunk, upper and lower extremities, rather than to individual motion units (Fig. 19). Using PET to measure regional cerebral blood flow (rCBF), Grafton et al. (1993) have shown within-arm somatotopy of the primary motor cortex, the SMA, and the CMA. Kleinschmidt et al. (1997) used fMRI to show somatotopy for digits in the human hand motor area and concluded that "… somatotopy within the hand area of the primary motor cortex does not present as qualitative functional segregation but as quantitative predominance of certain movement or digit representation embedded in an overall joint hand area" (Naidich et al. 2001b).

6.3 Selected Areas Involved in Motor and Speech Function

6.3.1 Primary Motor Cortex (M1)

The primary motor cortex is designated M1 and corresponds to BA 4. M1 extends from the anterior part of the paracentral lobule on the medial surface, over the cerebral margin, and down the convexity along the crown and posterior face of the precentral gyrus (Figs. 3 and 17). Its anteroposterior extent is broader superiorly and on the medial surface. From there, BA 4 tapers progressively downward toward the sylvian fissure. Just above the sylvian fissure and behind the inferior frontal gyrus, BA 4 becomes restricted to a narrow strip along the posterior face of the precentral gyrus, within the central sulcus (Fig. 17).

M1 is heterotypical agranular isocortex characterized by significant overall cortical thickness, reduced to absent granule cells in layer IV, prominent pyramidal cells in layers III and V, and prominent giant Betz cells in lower layer V (Zilles et al. 1996). The individual Betz cells are largest in size superomedially at the paracentral lobule and smallest inferolaterally at the operculum (Carpenter and Sutin 1983). Classically, the somatotopy of M1 is given by the motor homunculus (Fig. 18). Each functional zone was considered to be responsible for directing the action of a group of muscles that effects motion across a joint. Individual neurons within this group innervate different muscles, so that individual muscles are innervated repeatedly in different combinations by multiple different cell clusters to effect action across different joints. In the classic concept, therefore, the

motor map represents motion of the joint, rather than any single body part. More recently, Graziano et al. (2002) have shown that the motor homunculus may better be considered a map of final body postures.

M1 activates anterior horn cells within the spinal cord to generate specific patterns of movement (Marsden et al. 1996). It serves to execute voluntary activity of the limbs, head, face, and larynx, both contralaterally and ipsilaterally. Contralaterally, M1 excites all muscle groups of the extremity. Ipsilaterally, M1 excites the proximal musculature most strongly, especially the shoulder. By direct stimulation of neurons in monkeys, Tanji et al. (1987, 1988) found that 77.2 % of movement-related M1 neurons are contralateral motor neurons, affecting action of the contralateral side, 8.2 % are ipsilateral motor neurons, responsible for action on the ipsilateral side, and 4.5 % are bilateral motor neurons. Stimulation of M1 produces simple motions, such as flexion and extension at one or more joints, and not skilled movements. Regions of M1 exhibit different thresholds for inciting action. These thresholds are lowest for the thumb and highest for the face.

Activation studies confirm activation of the ipsilateral hemisphere by sensorimotor tasks (Li et al. 1996). The ipsilateral activation is greater for motor than for sensory tasks and is greater for the nondominant hand than for the dominant hand (Li et al. 1996). The left and the right primary motor cortices show reciprocal actions. Transcranial magnetic stimulation of the motor cortex may inhibit the contralateral cortex (Allison et al. 2000). Direct focal stimulation of M1 causes excitation of a homologous area in the contralateral M1, surrounded by a zone of inhibition (Allison et al. 2000; Asanuma and Okuda 1962). In fMRI studies, unilateral finger movements activate M1 ipsilaterally. The same movements may also deactivate portions of M1 ipsilaterally (Allison et al. 2000).

6.3.2 Supplementary Motor Area (SMA)

The SMA (Figs. 18 and 19) (Penfield and Welch 1951) is also known by a large number of synonyms, including the SMA proper, caudal SMA, posterior SMA, the supplementary sensorimotor area, M2, and BA 6a α (medial) (Olivier 1996; Rizzolatti et al. 1996; Seitz et al. 1996). In this chapter, the term SMA refers to the SMA proper, distinct from the more anteriorly situated pre-SMA. Anatomically, the SMA proper corresponds to BA 6a α (medial) situated along the medial cerebral cortex in the paracentral lobule and posterior portion of the superior (medial) frontal gyrus. Its specific site varies among individuals, but it is typically found in relation to the medial precentral sulcus (Zilles et al. 1996). Zilles et al. (1996) report that the SMA is located between the VAC and the VPC (Fig. 20).

The SMA is bordered anteriorly by the pre-SMA, posteriorly by the primary motor cortex, laterally by the premotor cortex on the convexity, and ventrally (inferiorly) by the posterior CMA (Fried 1996; Zilles et al. 1996).

The SMA is a heterotypical agranular isocortex characterized by reduced to absent granule cell layers and by absence of Betz cells in pyramidal cell layer V. The SMA (BA 6a α on the medial surface) can be distinguished from the laterally adjacent premotor area (BA 6a α on the convexity), because the SMA has increased cell density in the lower part of layer III and in layer Va (Zilles et al. 1996). The SMA can be distinguished from the pre-SMA, because the SMA shows poorer delineation of the laminae and poorer distinction of layer III from layer V (Zilles et al. 1996).

The SMA exhibits crude somatotopy. From anterior to posterior, one finds representations of the head, trunk, and upper and lower extremities (Fried et al. 1991). In humans, one stimulation study with subdural electrode grids placed along the mesial cortex elicited a finer somatotopy (Fried et al. 1991). In order from anterior to posterior, these authors found the face, neck, distal upper extremity, proximal upper extremity, proximal lower extremity, and distal lower extremity. The SMA clearly shows greater representation of the contralateral side than the ipsilateral side. The dominant SMA exerts more control than the nondominant SMA, both contralaterally and ipsilaterally. The supplementary eye fields lie in relation to the head portion of the SMA but are distinct from the SMA (Lim et al. 1996; Tanji 1994).

The SMA appears to act in several different ways:

- *Connections to the Cervical Motor Neurons.* The SMA has tight, probably monosynaptic, connections to the cervical motoneurons (94 % contralateral, 6 % ipsilateral). SMA activity in one hemisphere is associated with movement of either arm, especially whole-arm prehension involving the shoulder and trunk muscles. Stimulation of the SMA causes a characteristic posture with raising of the opposite arm (abduction and external rotation at the shoulder with flexion at the elbow) and turning of the head and eyes to gaze at the elevated hand (Carpenter and Sutin 1983; Chauvel et al. 1996; Freund 1996a, b). The trunk and lower extremities show bilateral synergic contractions (Carpenter and Sutin 1983). Distal hand muscles are weakly represented in the SMA. Isolated finger movements, easily elicited by stimulation of MI, are rarely elicited by stimulating SMA. The SMA appears less involved with distal grasping.

- *Posture.* The SMA plays a role in posture, especially in anticipating and correcting posture during motor tasks, so that the final position or task is performed successfully. In normal subjects, when a heavy object is lifted from one hand by the other, there is anticipatory adjustment of the posture of the forearm flexors, so position is maintained despite the unloading (Brust 1996; Viallet et al. 1992).

- *Action.* Stimulation of the SMA leads to an urge to act and an anticipation of action (Fried et al. 1991). In monkeys,
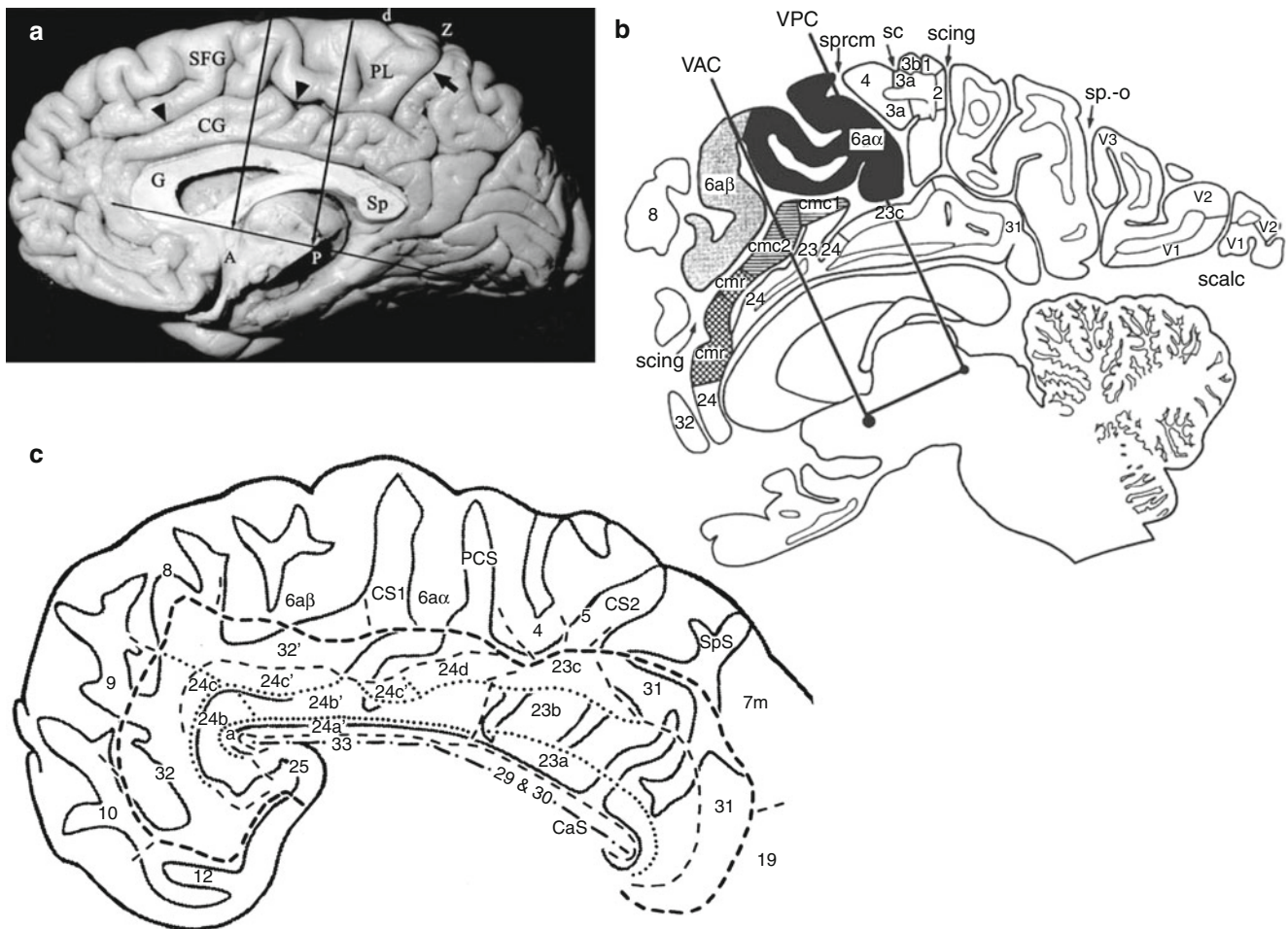
Fig. 20 (**a–c**) Mesial motor areas: SMA, pre-SMA, and CMA. (**a**) Gross anatomy of the medial surface of the hemisphere. Prepared specimen, oriented with anterior to the reader's left. This hemisphere displays the co-curvilinearity of the fornix (*F*), the genu (*G*), and splenium (*Sp*) of the corpus callosum; the callosal sulcus (not labeled), the cingulate gyrus (*CG*); the single cingulate sulcus (*arrowheads*); the superior frontal gyrus (*SFG*); and the paracentral lobule (*PL*). The pars marginalis (*arrow*, *z*) of the cingulate sulcus sweeps upward to the cerebral margin to define the posterior aspect of the paracentral lobule. The central sulcus (*d*) cuts the cerebral margin just anterior to the pars marginalis and then courses a short (and variable) distance down the medial face of the paracentral lobule, almost perpendicular to the pars marginalis. To illustrate the anatomic relationships, the AC-PC line has been drawn from the superior surface of the anterior commissure (AC, here labeled *A*) to the inferior surface of the posterior commissure (PC, here labeled *P*) and the perpendiculars erected to this line at the AC and the PC. The AC-PC line is the baseline for the Talairach-Tournoux coordinate system (Talairach and Tournoux 1988). (**b**) The medial parasagittal plane, oriented with anterior to the readers' left. *CC* corpus callosum,

AC anterior commissure, *PC* posterior commissure. The VAC and VPC are the vertical lines erected perpendicular to the AC-PC line at AC (*VAC*) and PC (*VPC*). The cytoarchitectonic areas are numbered after Brodmann and the Vogts. *Black areas* show the position of the SMA on the medial surface of the hemisphere. *Solid gray* shows the position of the pre-SMA. *Cross hatching* indicates the rostral portion of the cingulate motor area (*cmr*), whereas the *horizontal lines* show the caudal portion of the cingulate motor area (*cmc*), itself divided into parts one and two. *scing* cingulate sulcus, *sc* central sulcus. *V1–V3* are the visual cortical areas. (**c**) Flat map of the cytoarchitectonic areas of the human cingulate cortex and the locations of adjacent areas. The cingulate sulcus is shown with two separate segments (*CS1*, *CS2*). *Thick lines* outline of the cingulate areas, *thin lines* divide each major cingulate area, *stippling* borders of each sulcus, *dotted lines* the subdivisions of each area, *dot-dash line* the fundus of the callosal sulcus; the fundi of the other sulci are not marked for simplicity. *PCS* paracentral sulcus (**a** From Naidich et al. (2001); **b** From Zilles et al. (1996) and Vogt et al. (1997); **c** Adapted from Vogt et al. (1995); with permission)

Tanji et al. (1987, 1988) used intracellular recording to demonstrate that 38 % of SMA cells fire before any action is performed. At least some SMA neurons fire before M1 neurons.

- *Laterality*. The SMA is involved with selecting the laterality of the task. In monkeys, 27 % of motor-related SMA neurons only fire before deciding on which side to perform an

action (Tanji et al. 1987, 1988). Considering SMA neurons and premotor neurons together as one group of non-M1 neurons, Tanji et al. (1987, 1988) showed that when choosing which upper extremity to use for a job, 16 % of non-M1 cells fire before deciding right, not both; 20 % fire before deciding left, not both; 20 % fire before deciding either, not both; and 40 % fire before deciding both, not either.

- *Coordination and Cooperation*. The SMA serves to assist bimanual coordination and cooperation between the paired upper and the paired lower extremities, especially for self-initiated action. The SMA appears to be required for independent control of the contralateral hand.
- *Sequences of Action*. The SMA is heavily involved in learning and generating sequences of actions and with executing multiple actions involving both sides of the body (Gilman and Newman 1996; Passingham 1996; Shibasaki et al. 1993). It may serve in selecting a specific action from among a group of remembered tasks. In monkeys, Tanji and Shima (1994) found one group of SMA cells that were preferentially activated in relation to a particular order of forthcoming movements, guided by memory. A second group of SMA cells became active after the performance of one particular movement and then remained active during the waiting period before performing a second specific movement. These cells were not active if the preceding or subsequent movement was different. Thus, these cells seem to signal a temporal linkage combining two specific movements (Tanji and Shima 1994). Single unit discharges were also observed in the SMA before the performance of the remembered sequence of movements (preparatory sequencing of neurons) and in the midst of the sequence of movements (tonic sequencing of neurons) (Tanji 1994; Tanji et al. 1987, 1988; Tanji and Shima 1994). Similarly, rCBF in the SMA increases with ideation about sequential motor tasks (e.g., when subjects plan but do not execute fast, isolated finger movements) (Roland 1999). When these tasks are actually executed, increased rCBF can be seen contralaterally in M1 and bilaterally in the SMA. From these data, the SMA seems to be crucial for learned, internally generated (i.e., self-initiated) voluntary motor behavior (Burton et al. 1996; Freund 1996a, b; Freund and Hummelsheim 1985; Rao et al. 1993), especially in the preparation and initiation of such voluntary motor behavior (Freund 1996b; Luders 1996). The SMA seems to be less related to performance of the movements themselves. Simple repetition of fast finger motion does not stimulate SMA (Freund 1996b).

  Stimulation studies also show a relation between the complexity of a task and the speed with which the action itself is performed. Simple tasks, like flexion of one joint, are commonly performed rapidly. More complex tasks involving multiple joints, multiple body regions, or both evolve more slowly. In some stimulations, the responses elicited were repeated several times until stimulation stopped (Fried 1996).

- *Attention-Intention Network*. The SMA may form part of an attention-intention network. Fried (1996) found that most ipsilateral and bilateral sequences can be elicited from the right, nondominant SMA. The right hemisphere

has an attention mechanism that spans both hemispheres, whereas the left hemisphere seems to mediate only contralateral attention (Fried et al. 1991). Therefore, the lateralization of attention to the right hemisphere and the lateralization of motor intention to the right SMA may signify a right cerebral dominance for attention and motor intention directed at the external milieu in which the motor action takes place (Fried 1996; Fried et al. 1991; Naidich et al. 2001b).

6.3.3 Pre-supplementary Motor Area (Pre-SMA)

The term pre-SMA signifies a motor area that has also been called rostral SMA, anterior SMA, BA 6a β (medial), and the supplementary negative motor area (Figs. 19 and 20). It corresponds to BA 6a β (medial) (Seitz et al. 1996). The pre-SMA lies along the medial face of the superior (medial) frontal gyrus just anterior to the SMA. It shows individual variability. According to Zilles et al. (1996), the pre-SMA lies predominantly anterior to VAC (Fig. 20). It borders posteriorly on the SMA, laterally on the anterior portion of the premotor cortex on the convexity and ventrally (inferiorly) on the anterior cingulate motor area (Zilles et al. 1996).

The pre-SMA is heterotypical agranular isocortex with no Betz cells. It can be distinguished from the SMA posterior to it because the pre-SMA has more pronounced lamination and clearer demarcation of layer III from layer V (Zilles et al. 1996). The pre-SMA exhibits a somatotopy similar in form to the SMA, but even cruder in detail. From anterior to posterior, there are areas for the head and upper and lower extremities.

The pre-SMA seems to serve in sequencing and preparing complex tasks, especially internally generated, visually guided tasks. Stimulation of the pre-SMA may elicit negative motor activity for diverse tasks. Fried (1996) found that pre-SMA stimulation causes slowing or arrest of the entire spectrum of motor activity tested, including speech. When a patient executes a repetitive task, such as rapid alternating movements of the hand, stimulation of the pre-SMA causes the movements to gradually slow down and come to a halt. Activation studies suggest that the pre-SMA is involved in the decision whether to act, whereas the SMA proper plays a similar role in directing motor action once the decision to act is made (Humberstone et al. 1997; Naidich et al. 2001b).

6.3.4 Cingulate Motor Area (CMA)

The CMA is composed of two portions (Fig. 20), which appear to correspond to the functionally defined anterior cingulate motor area (CMA rostral; cmr) and a posterior cingulate motor area (CMA caudal; cmc). The CMA corresponds to BA 24c and BA 24d (and perhaps the posterior portion of BA 32, BA 32′ of Vogt) (Vogt and Vogt 1919, 1926). It lies in the superior (dorsal) and inferior (ventral) banks of the

cingulate sulcus and, in macaques, does not extend onto the medial surface of the cingulate gyrus (Shima et al. 1991). From the callosal sulcus (inferiorly) to the superior frontal gyrus (superiorly), the cerebral cortex undergoes transition from true allocortex (BA 33), through intermediate stages (lower and upper BA 24), to true isocortex (BA 32) (Zilles et al. 1996). Intermediate area BA 24, therefore, is subdivided into three bands coextensive with the cingulate gyrus and sulcus. These three bands area designated BA 24a (ventral band), 24b (intermediate band), and 24c and 24d (dorsal bands). BA 32 lies superior to BA 24c and BA 24d. Dorsal bands BA 24c and 24d are then subdivided further into a rostral zone (cmr), conforming approximately to BA 24c, and a caudal zone (cmc) conforming approximately to BA 24d (Vogt et al. 1995, 1997; Zilles et al. 1996). The cmr lies entirely rostral to VAC. The cmc flanks VAC but lies entirely anterior to the VPC (Fig. 20).

BA 24c and 24d (cmr and cmc) are heterotypical agranular motor cortices (Zilles et al. 1996). In fine detail, both cmr and cmc appear heterogeneous, leading to further subdivisions of their cytoarchitecture and nomenclature (Zilles et al. 1996). Compared with BA 24c, BA 24d shows a thinner overall width of layer V, clearer borders between layers III and V, larger cells in layers III and VI, and, larger cells in layer V.

The CMA exhibits crude somatotopy with multiple representations of the body (Freund 1996b). BA 24c includes representations of the head and the forelimbs (Freund 1996b). Posterior to BA 24c, BA 24d has representations for the forelimbs and the hindlimbs, but with the forelimbs situated caudal to the hindlimbs (Luppino et al. 1991). Thus, the CMA (cmr and cmc) exhibits mixed somatotopy that is partially reversed from that seen in the SMA and in the pre-SMA (Freund 1996b; Luppino et al. 1991; Zilles et al. 1996).

The CMA projects directly to M1 with somatotopic organization (Shima et al. 1991). CMA fibers also project directly to the spinal cord (Shima et al. 1991). Stimulation of the CMA causes contralateral or bilateral movements of the lower and the upper extremities (Freund 1996b). Single-cell studies in macaques show that more than 60 % of CMA motoneurons fire before movement-related activity (Shima et al. 1991). Most are involved in simple movements of the distal forelimb. These cells may show either a short lead time or a long lead time between firing and action. Long lead time cells (500 ms to 2 s) are more common in the anterior than the posterior cingulate area and show this long lead time in response to self-paced tasks, not stimulus-triggered tasks. Few CMA cells respond to visual, auditory, or tactile stimuli. Overall, the anterior CMA appears to be significant for self-paced internally guided tasks. According to Paus et al. (1993), the anterior CMA participates in motor control by facilitating the execution of appropriate responses or by suppressing the execution of inappropriate responses.

The zone designated rostral CMA (cmr) is involved with autonomic function. Cells project to the hypothalamus and periaqueductal gray matter. Stimulation of cmr causes non-volitional vocalization and fear reactions involving the heart, gut, bladder, and genitalia (Jurgens 1983; Nimchinsky et al. 1995, 1997; Naidich et al. 2001b; Vogt et al. 1995, 1997).

6.3.5 Premotor Area

The premotor area (pre-MA) may be designated M2. It extends along the frontal convexity to occupy contiguous portions of the superior frontal gyrus, the middle frontal gyrus, and the precentral gyrus (Figs. 19 and 20). The dorsal pre-MA lies within the posterior portions of the superior and middle frontal gyri. The ventral pre-MA occupies the anterior face and part of the crown of the precentral gyrus anterior to the primary motor area (M1). Like M1, the ventral portion of pre-MA progressively tapers inferiorly. An additional small area, BA 6b, lies further inferiorly, superior to the sylvian fissure and anterior to the motor face area. The pre-MA corresponds to BA 6a α (convexity), BA 6a β (convexity), and BA 6b (Carpenter and Sutin 1983).

The pre-MA is a heterotypical agranular isocortex with large, well-formed pyramidal cells in layers III and V. Betz cells are absent. Large pyramidal cells that resemble Betz cells are present in the border zone abutting onto BA 4 posteriorly, but these cannot be designated Betz cells, by definition. Granule cell layer IV is thin and difficult to discern. The pre-MA exhibits somatotopy that is similar to, but cruder than, the motor homunculus of the primary motor cortex (M1; BA 4).

Stimulation of BA 6a α (convexity) causes responses similar to those elicited by stimulation of the primary motor cortex M1 (BA 4) but requires higher current to elicit the response. Stimulation of BA 6a β (convexity) elicits more general movement patterns, characterized by abduction and elevation of the arm (frequently associated with rotation of the head, eyes, and trunk to the opposite side). Stimulation of the leg region causes synergic patterns of flexion and extension of the contralateral extremity (Carpenter and Sutin 1983; Freund 1996a). These movements resemble the effect of stimulating the SMA (Freund 1996a). Stimulation of BA 6b produces rhythmic, coordinated, complex movements of the face, masticatory, and laryngeal and pharyngeal musculature (Carpenter and Sutin 1983). Like the pre-SMA, the pre-MA contains cells that fire before a motion is initiated and that appear to determine the usage of the extremities: right, left, or both (Tanji et al. 1987, 1988). Intracellular recordings in monkeys indicate that 48 % of motor-related pre-MA neurons fire before all types of motion. Of motor-related pre-MA neurons, 18 % fire exclusively before decisions as to the laterality of subsequent activity, not in relation to the performance of the movement (Tanji et al. 1987, 1988). The pre-MA responds more to visual signals and is active in

visually guided sequential movements. The pre-MA appears active (1) during mental preparation for a motor task directed by verbal instructions; (2) when voluntary movements are performed under somatosensory, auditory, or visual guidance; and (3) when sensory input is necessary to execute the task. The pre-MA appears especially active when a new motor program is established or an old motor program is modified on the basis of new sensory input (Roland et al. 1980a, b). In monkeys, some of the neurons seem to be stimulated both in performing a task and in observing a similar task being performed by the experimenter (especially when the monkey uses manual or oral "observation"). These neurons are designated mirror neurons (Gallese et al. 1996; Naidich et al. 2001b).

6.3.6 Prefrontal Cortex (Pre-FC)

The term prefrontal cortex designates the cortex that is situated anterior to the pre-MA, corresponding to BA 9, BA 10, and BA 46. It lies along the frontal convexity in the superior and middle frontal gyri and extends onto the medial surface of the frontal lobe along the superior (medial) frontal gyrus (Figs. 3, 16, and 17). The pre-FC is a homolateral frontal type of isocortex characterized by a more-or-less clearly recognizable granule cell layer IV and an absence of Betz cells (Zilles et al. 1996). No somatotopy is known.

The pre-FC is involved with executive functions, behavior, and memory. Brodmann's area 46 on the dorsolateral pre-FC appears to be involved with the selection of items, whether selecting different items from an internal memory of possible tasks or selecting freely between movements needed to perform a voluntary action (Rowe et al. 2000). Right dorsolateral pre-FC (BA 9 and BA 46) is involved in decisions of what to do and when to do it (Marsden et al. 1996; Passingham 1996). Neurons of the pre-FC are involved with inhibitory responses to stimuli that require a delay in the motor responses (Gilman and Newman 1996). They are thought to integrate motivational elements with complex sensorimotor stimuli (Gilman and Newman 1996). Hasegawa et al. (2000) have detected pre-FC neurons that appear to track long periods of time (as long as 30 s). Activity of these cells correlates with success of past or future performance of complex tasks, not the immediate activity. These cells may set the tone for general behavior, in a fashion similar to that accomplished by stimulants, enthusiasm, arousal, or fatigue (Hasegawa et al. 2000). Using PET measurement of rCBF during a simple motor task of sequential opposition of the thumb to each finger, Kawashima et al. (1993) showed activation of the contralateral pre-FC for both right- and left-handed tasks. Tasks performed with the nondominant hand, however, additionally activated the ipsilateral primary motor area and ipsilateral pre-FC. Thus, the pre-FC exhibits asymmetric activity with dominant or nondominant simple motor tasks (Naidich et al. 2001b).

6.3.7 Broca's Area

Broca's area is the motor speech area. It conforms to BA 44 and to the posterior portion of BA 45. Broca's area occupies the inferior frontal gyrus (*pars opercularis* and a small posterior portion of *pars triangularis*) in the dominant hemisphere. Some data indicate that many women, but not men, have motor speech areas in the inferior frontal gyri bilaterally (Pugh et al. 1996; Shaywitz et al. 1995). The motor speech area traditionally assigned to the inferior frontal gyrus has recently been suggested to lie instead in the anterior insula (Price 2000). Broca's area is a heterotypical agranular isocortex, characterized by reduced thickness of the granule cell layer IV and by the presence of large pyramidal cells in layers III and V. Betz cells are absent. No somatotopy is known.

Broca's area is believed to generate the signals for the musculature to produce meaningful sound. It may also be involved in the initiation of speech (Alexander et al. 1989; Demonet et al. 1992), the organization of articulatory sequences (Demonet et al. 1992), and in the covert formation of speech (inner speech). Lesions of Broca's area are associated with a form of aphasia termed, variably, motor aphasia, anterior aphasia, non-fluent aphasia, executive aphasia, and Broca's aphasia. Patients who have this form of aphasia exhibit difficulty with the production of speech and, therefore, produce little speech. The speech produced is emitted slowly, with great effort and with poor articulation (Geschwind 1970). There are phonemic deficits. Small grammatical words and word endings are omitted (Geschwind 1970). There is a characteristic, comparable disorder in their written output. Surprisingly, these patients may retain musical ability and, despite severe motor aphasia, may sing melodies correctly and even elegantly (Geschwind 1970). Patients who have Broca's aphasia maintain good comprehension of the spoken and written language. Patients who have lesions restricted to the traditional Broca's area in the inferior frontal gyrus do not exhibit persisting speech apraxia (Dronkers 1996). Recovery after Broca's aphasia appears to involve a transient shift of function to the right hemisphere, followed by a return to normal laterality (Neville and Bavelier 1998). A new capability for speech production has been observed to arise within the right hemisphere of an adult several years after corpus callosotomy (Neville and Bavelier 1998).

Broca's area and its right hemispheric homologue are also involved with auditory hallucinations (Cleghorn et al. 1990; Lennox et al. 2000; Mcguire et al. 1993). Schizophrenics experiencing auditory hallucinations show increased metabolism and activation in Broca's area, the left anterior cingulate region, and the left and right superior temporal regions, among other sites (Cleghorn et al. 1990; Lennox et al. 2000; Mcguire et al. 1993).
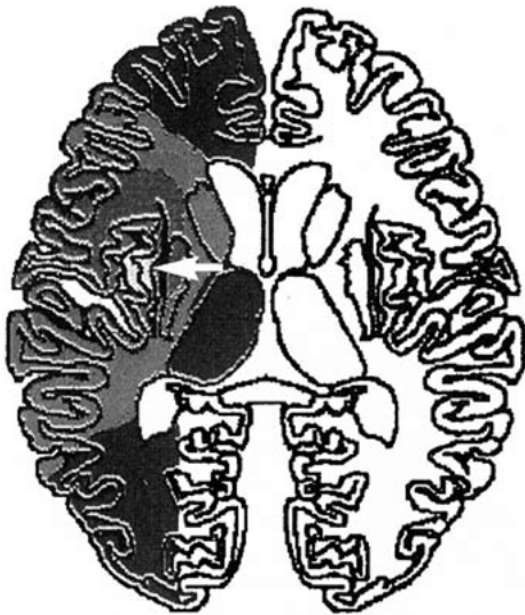
Fig. 21 Speech apraxia. Complete double dissociation in Dronkers' area. Pooled data from 25 patients with speech apraxia show that the only region of involvement common to all cases is the precentral gyrus (*white arrow*) of the insula. Pooled data from 19 other patients with similar infarctions but no speech apraxia showed no involvement in this same area (From Dronkers (1996); with permission)

6.3.8 Dronkers' Area

Dronkers' area (Dronkers 1996) has no other specific designation. Brodmann did neither parcelate nor number the insular cortex in his final work. Dronkers' area occupies the precentral gyrus of the anterior lobule of the insula. The cortex is a heterotypical agranular isocortex, characterized by a poorly defined layer IV and medium-sized pyramids in layers III and V. No somatotopy has yet been established.

Electrocortical stimulation of the insula during epilepsy surgery has been reported to cause word finding difficulties, but the specific site on the insula was not specified (Ojemann and Whitaker 1978). The anterior insula has been suggested to be the true site of the function that Broca ascribed to the inferior frontal gyrus (Price 2000). Lesions of the precentral gyrus of the insula are associated with speech apraxia (Fig. 21). This is a disorder of the motor planning of speech, i.e., a disorder in programming the speech musculature to produce correct sounds in the correct order with the correct timing (Dronkers 1996). Such patients exhibit inconsistent articulatory errors that approximate the target word. They grope toward the desired word with disruption of prosody and rate (Dronkers 1996). These patients maintain good perception of language and can perceive and recognize speech sounds, including their own articulatory errors.

An alternate conception of speech apraxia is that it represents a disorder in temporal coordination that disrupts the timing or the integration of movements between two independent articulators. Speech apraxia is distinct from oral apraxia. Oral apraxia is a defect in planning and performing voluntary oral movements with the muscles of the larynx, pharynx, lips, and cheeks, although automatic movements of the same muscles are preserved (Tognola and Vignolo 1980). Oral apraxia often coexists with speech apraxia and has been related to lesions in the left frontal and central opercula, in the anterior insula, and in a small area of the STG (Dronkers 1996; Tognola and Vignolo 1980). The insula has also been reported to be involved in conductive aphasia and Broca's aphasia, where articulatory errors are prominent (Dronkers 1996).

6.3.9 Sensory Appreciation of Speech

The sensory speech area may be designated Wernicke's area (WA). The site(s) of Wernicke's area are very poorly defined (Roland 1999). Most of WA appears to lie along the most caudal part of BA 22 in the STG and the planum temporale (area tpt of Galaburda and Sanides 1980) or TA 1 of Von Economo and Koskinas (1925). Wernicke's area also includes part of the multimodal belt in the STS (Nieuwenhuys 1994; Nieuwenhuys et al. 1988). Thus, one may also include in WA BA 40, BA 39, BA 22, and BA 37. Anatomically, WA is the least well-defined area, largely due to the significant variation in gyral and sulcal anatomy of this region of the brain (von Economo and Koskinas 1925). In most individuals, WA involves parts of the dominant hemisphere around the posterior sylvian fissure, i.e., the SMG, the angular gyrus, the bases of the STG and the MTG, and the planum temporale. Price reports that the role ascribed by Wernicke to WA is actually found along the posterior superior TS (Price 2000). Cytoarchitectonically, Wernicke's area is a homotypical granular cortex.

Wernicke's area serves to recognize speech relayed to it from the left HG. Direct cortical stimulation of WA intraoperatively causes impairment of language (Ojemann 1983; Ojemann and Whitaker 1978; Ojemann et al. 1989). Patients who have lesions in WA exhibit a form of aphasia designated, variably, sensory aphasia, fluent aphasia, posterior aphasia, and Wernicke's aphasia. These patients produce speech fluently, effortlessly, and rapidly, often too rapidly. The output has the rhythm and melody of normal speech but is remarkably empty of content. These patients show poor comprehension of language and poor ability to repeat language. They use poor grammar and exhibit many errors in word usage (termed *paraphrasias*), including well-articulated replacements of simple sounds, such as spoot for spoon (Geschwind 1970). Patients who have Wernicke's aphasia show the same errors in written output. Recovery of function after Wernicke's aphasia appears to involve a long-lasting shift of function to the right hemisphere (Naidich et al. 2001a).
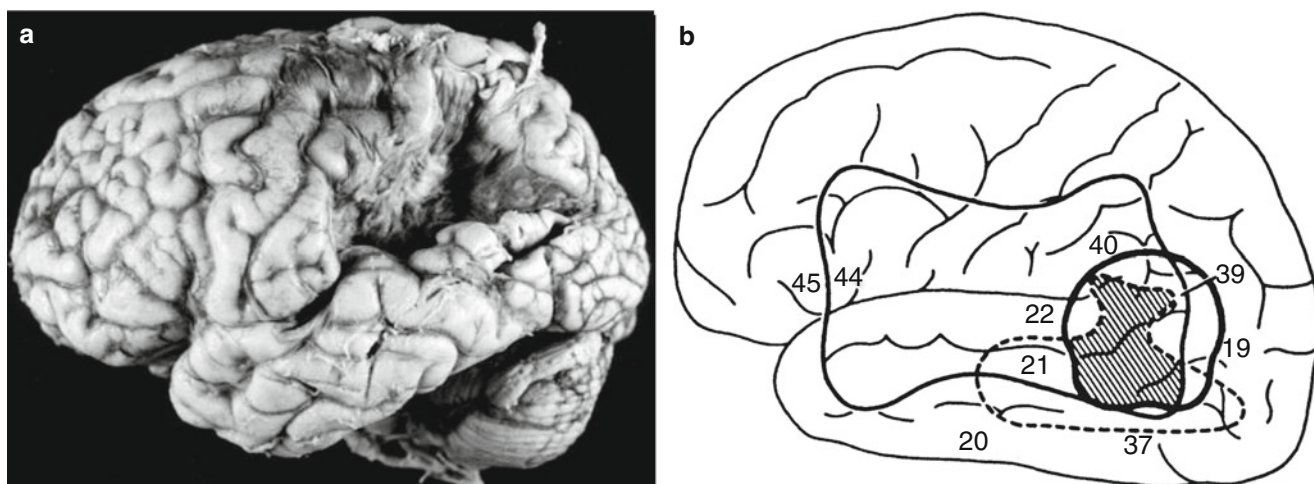
Fig. 22 (**a**, **b**) Lesions of the posterior language area. (**a**) Large depressed area representing an old infarction of the temporoparietal language area in the dominant left hemisphere. (**b**) Site of pure semantic deficit for single word comprehension. Area of *broken line* indicates the cortical projection of an extensive subcortical hematoma cavity (From Hart and Gordon (1990); with permission)

6.3.10 Interconnection of Speech Areas: Arcuate Fasciculus

The term *arcuate fasciculus* signifies a broad bundle of fibers that interconnects WA with Broca's area. The arcuate fasciculus may also be designated the anterior limb of the superior longitudinal fasciculus (Nieuwenhuys et al. 1988). It extends between BA 22 and BA 44. The arcuate fasciculus courses from the posterior temporal lobe around the posterior edge of the sylvian fissure to the inferior parietal lobule deep to the SMG and then forward deep to the insula to reach the inferior frontal gyrus. More rostral parts of the STG are also connected with successively more rostral parts of the prefrontal cortex (Nieuwenhuys et al. 1988). The temporal pole is connected with the medial frontal and orbitofrontal cortices through the uncinate fasciculus (Nieuwenhuys et al. 1988). The auditory association areas, particularly the rostral areas, establish connections with the paralimbic cortex of the cingulate gyrus and the PHG (Nieuwenhuys et al. 1988). No myelototopy has yet been determined.

Lesions of the arcuate fasciculus disconnect Wernicke's area from Broca's area, causing a conduction aphasia (Figs. 22 and 23). Patients who have conduction aphasia exhibit good comprehension of the spoken language (WA intact) and fluency of speech (Broca's area intact) but have phonetic errors and poor ability to repeat language. The patient has fluent paraphasic speech and writing with good comprehension of spoken and written language (Geschwind 1970). The inability to repeat speech indicates disruption of the arcuate fasciculus. The disorder in repetition is greatest for the small grammatical words (the, if, is). Repetition of numbers is relatively preserved (Naidich et al. 2001a).

Fig. 23 The arcuate fasciculus interconnects the language areas. Immediately deep to the gyri and sulci of the language areas lie interconnecting fiber tracts, specifically, the arcuate fasciculus (*1*), extreme capsule (*2*), inferior longitudinal fasciculus (*5*), short association fibers (*6*), superior longitudinal fasciculus (*7*), and uncinate fasciculus (*9*); (*8*) = temporal pole (From England and Wakely (1991), p 95, with permission)

Conclusion

Understanding of the structure and function of the brain depends, in part, on an understanding of the basic anatomic structure of the parts, the cytoarchitecture of the cortex, the functional somatotopy, and the interconnections and dominances among the diverse regions. This chapter has tried to present some of the relevant data and to provide a guide to our current, necessarily limited, understanding of brain function. It is hoped that it may serve as one foundation for advances in understanding the brain.

References

Albanese E, Merlo A, Albanese A, Gomez E (1989) Anterior speech region. Asymmetry and weight-surface correlation. Arch Neurol 46:307–310

Alexander MP, Hiltbrunner B, Fischer RS (1989) Distributed anatomy of transcortical sensory aphasia. Arch Neurol 46:885–892

Allison JD, Meador KJ, Loring DW, Figueroa RE, Wright JC (2000) Functional MRI cerebral activation and deactivation during finger movement. Neurology 54:135–142

Asanuma H, Okuda O (1962) Effects of transcallosal volleys on pyramidal tract cell activity of cat. J Neurophysiol 25:198–208

Brodmann K (1909) Vergleichende Lokalisationlehre der Grosshirnrinde. Verlag von Johann Ambrosius Barth, Leipzig

Brust JC (1996) Lesions of the supplementary motor area. Adv Neurol 70:237–248

Burton DB, Chelune GJ, Naugle RI, Bleasel A (1996) Neurocognitive studies in patients with supplementary sensorimotor area lesions. Adv Neurol 70:249–261

Carpenter MB, Sutin J (1983) Human neuroanatomy. In the cerebral cortex. Williams and Wilkins, Baltimore, pp 643–705

Chauvel PY, Rey M, Buser P, Bancaud J (1996) What stimulation of the supplementary motor area in humans tells about its functional organization. Adv Neurol 70:199–209

Cleghorn JM, Garnett ES, Nahmias C, Brown GM, Kaplan RD, Szechtman H et al (1990) Regional brain metabolism during auditory hallucinations in chronic schizophrenia. Br J Psychiatry 157:562–570

Daniels OL, Haughton VM, Naidich TP (1987) Cranial and spinal magnetic resonance imaging. An atlas and guide. Raven Press, New York

Dejerine J (1895) Anatomie des centres nerveux. Rueff et Cie, Paris

Demonet JF, Chollet F, Ramsay S, Cardebat D, Nespoulous JL, Wise R et al (1992) The anatomy of phonological and semantic processing in normal subjects. Brain 115:1753–1768

Dronkers NF (1996) A new brain region for coordinating speech articulation. Nature 384:159–161

Duvernoy H (1991) The human brain: surface. Three-dimensional sectional anatomy and MRI. Springer, Berlin

England MA, Wakely J (1991) Color atlas of the brain and spinal cord. Mosby Year Book, St Louis

Freund HJ (1996a) Functional organization of the human supplementary motor area and dorsolateral premotor cortex. Adv Neurol 70:263–269

Freund HJ (1996b) Historical overview. Adv Neurol 70:17–27

Freund HJ, Hummelsheim H (1985) Lesions of premotor cortex in man. Brain 108:697–733

Fried I (1996) Electrical stimulation of the supplementary sensorimotor area. Adv Neurol 70:177–185

Fried I, Katz A, McCarthy G, Sass KJ, Williamson P, Spencer SS et al (1991) Functional organization of human supplementary motor cortex studied by electrical stimulation. J Neurosci 11:3656–3666

Galaburda A, Sanides F (1980) Cytoarchitectonic organization of the human auditory cortex. J Comp Neurol 190:597–610

Galaburda AM, LeMay M, Kemper TL (1998) Right-left asymmetries in the brain. Structural differences between the hemispheres may underlie cerebral dominance. Science 199:852–856

Gallese V, Fadiga L, Fogassi L, Rizzolatti G (1996) Action recognition in the premotor cortex. Brain 119:593–609

Gannon PJ, Holloway RL, Broadfield DC, Braun AR (1998) Asymmetry of chimpanzee planum temporale: humanlike pattern of Wernicke's brain language area homolog. Science 279:220–222

Geschwind N (1965a) Disconnexion syndromes in animals and man. I. Brain 88:237–294

Geschwind N (1965b) Disconnexion syndromes in animals and man. II. Brain 88:585–644

Geschwind N (1970) The organization of language and the brain. Language disorders after brain damage help in elucidating the neural basis of verbal behavior. Science 170:940–944

Geschwind N, Levitsky W (1968) Human brain: left-right asymmetries in temporal speech region. Science 161:186–187

Gilman S, Newman SW (1996) Manter and Gatz's essentials of clinical neuroanatomy and neurophysiology. In the cerebral cortex. FA Davis, Philadelphia

Grafton ST, Woods RP, Mazziotta JC (1993) Within-arm somatotopy in human motor areas determined by positron emission tomography imaging of cerebral blood flow. Exp Brain Res 95:172–176

Graziano M, Taylor CS, Moore T (2002) Complex movements evoked by microstimulation of precentral cortex. Neuron 34:841–851

Gusmão S, Reis C, Tazinaffo U, Mendonça C, Silveira RL (2002) Definition of the anterolateral occipital lobe limit in anatomical specimens and image examination. Arq Neuropsiquiatr 60(1):41–46 (in Portuguese)

Hart J Jr, Gordon B (1990) Delineation of single-word semantic comprehension deficits in aphasia, with anatomical correlation. Ann Neurol 27:226–231

Hasegawa RP, Blitz AM, Geller NL, Goldberg ME (2000) Neurons in monkey prefrontal cortex that track past or predict future performance. Science 290:1786–1789

Humberstone M, Sawle GV, Clare S, Hykin J, Coxon R, Bowtell R et al (1997) Functional magnetic resonance imaging of single motor events reveals human presupplementary motor area. Ann Neurol 42:632–637

Iwasaki S, Nakagawa H, Fukusumi A, Kichikawa K, Kitamura K, Otsuji H et al (1991) Identification of pre- and postcentral gyri on CT and MR images on the basis of the medullary pattern of cerebral white matter. Radiology 179:207–213

Jensen J (1871) Die Furchen und Windungen der menschlichen Großhirnhemisphären. Allgemeine Zeitschrift fur Psychiatrie und psychisch-gerichtliche Medizin 27:465–473

Jurgens U (1983) Afferent fibers to the cingular vocalization region in the squirrel monkey. Exp Neurol 80:395–409

Kawashima R, Yamada K, Kinomura S, Yamaguchi T, Matsui H, Yoshioka S et al (1993) Regional cerebral blood flow changes of cortical motor areas and prefrontal areas in humans related to ipsilateral and contralateral hand movement. Brain Res 623:33–40

Kleinschmidt A, Nitschke MF, Frahm J (1997) Somatotopy in the human motor cortex hand area. A high-resolution functional MRI study. Eur J Neurosci 9:2178–2186

Kopp N, Michel F, Carrier H (1977) Etude de certaines asymetries hemispheriques du cerveau humain. J Neurol Sci 34:349–363

Korogi Y, Takahashi M, Okuda T, Ikeda S, Kitajima M, Yoshizumi K et al (1996) MR topography of the striate cortex: correlation with anatomic sections. Int J Neuroradiol 2:534–540

Lennox BR, Park SB, Medley I, Morris PG, Jones PB (2000) The functional anatomy of auditory hallucinations in schizophrenia. Psychiatry Res 100:13–20

Li A, Yetkin FZ, Cox R, Haughton VM (1996) Ipsilateral hemisphere activation during motor and sensory tasks. AJNR Am J Neuroradiol 17:651–655

Liegeois-Chauvel C, Musolino A, Chauvel P (1991) Localization of the primary auditory area in man. Brain 114:139–151

Liegeois-Chauvel C, Laguitton V, Badier JM, Schwartz D, Chauvel P (1995) Cortical mechanisms of auditive perception in man: contribution of cerebral potentials and evoked magnetic fields by auditive stimulations. Rev Neurol (Paris) 151:495–504

Lim SH, Dinner DS, Luders HO (1996) Cortical stimulation of the supplementary sensorimotor area. Adv Neurol 70:187–197

Luders HO (1996) The supplementary sensorimotor area. An overview. Adv Neurol 70:1–16

Luppino G, Matelli M, Camarda RM, Gallese V, Rizzolatti G (1991) Multiple representations of body movements in mesial area 6 and

the adjacent cingulate cortex: an intracortical microstimulation study in the macaque monkey. J Comp Neurol 311:463–482

Marsden CD, Deecke L, Freund HJ, Hallett M, Passingham RE, Shibasaki H et al (1996) The functions of the supplementary motor area. Summary of a workshop. Adv Neurol 70:477–487

McGuire PK, Shah GM, Murray RM (1993) Increased blood flow in Broca's area during auditory hallucinations in schizophrenia. Lancet 342:703–706

Meyer JR, Roychowdhury S, Russell EJ, Callahan C, Gitelman D, Mesulam MM (1996) Location of the central sulcus via cortical thickness of the precentral and postcentral gyri on MR. AJNR Am J Neuroradiol 17:1699–1706

Naidich TP, Brightbill TC (1995) The intraparietal sulcus. A landmark for localization of pathology on axial CT-scans. Int J Neuroradiol 1:3–16

Naidich TP, Brightbill TC (1996a) The pars marginalis: part 1. A "bracket" sign for the central sulcus in axial plane CT and MRI. Int J Neuroradiol 2:3–19

Naidich TP, Brightbill TC (1996b) Systems for localizing fronto-parietal gyri and sulci on axial CT and MRI. Int J Neuroradiol 2:313–338

Naidich TP, Matthews VP (2000) Integrating neuroanatomy and functional MR imaging: language lateralisation. ASNR AM Society Neuroradiol 75–83

Naidich TP, Valavanis AG, Kubik S (1995) Anatomic relationships along the low-middle convexity: part I – normal specimens and magnetic resonance imaging. Neurosurgery 36:517–532

Naidich TP, Valavanis AG, Kubik S (1997) Anatomic relationships along the low-middle convexity: part II – lesion localization. Int J Neuroradiol 3:393–409

Naidich TP, Hof PR, Gannon PJ, Yousry TA, Yousry I (2001a) Anatomic substrates of language. Neuroimaging Clin N Am 11:305–341

Naidich TP, Hof PR, Yousry TA, Yousry I (2001b) The motor cortex: anatomic substrates of function. Neuroimaging Clin N Am 11:171–193

Naidich TP, Kang E, Fatterpekar GM, Delman BN, Gultekin SH, Wolfe D et al (2004) The insula: anatomic study and MR imaging display at 1.5 T. AJNR Am J Neuroradiol 25:222–232

Neville HJ, Bavelier D (1998) Neural organization and plasticity of language. Curr Opin Neurobiol 8:254–258

Nieuwenhuys R (1994) The human brain: an introductory survey. Med Mundi 39:64–79

Nieuwenhuys R, Voogd J, van Huijzen C (1988) The human central nervous system. A synopsis and atlas. Springer, Berlin, pp 247–292

Nimchinsky EA, Vogt BA, Morrison JH, Hof PR (1995) Spindle neurons of the human anterior cingulate cortex. J Comp Neurol 355:27–37

Nimchinsky EA, Vogt BA, Morrison JH, Hof PR (1997) Neurofilament and calcium-binding proteins in the human cingulate cortex. J Comp Neurol 384:597–620

Ojemann GA (1983) Brain organization for language from the perspective of electrical stimulation mapping. Behav Brain Sci 6:189–230

Ojemann GA, Whitaker HA (1978) Language localization and variability. Brain Lang 6:239–260

Ojemann G, Ojemann J, Lettich E, Berger M (1989) Cortical language localization in left, dominant hemisphere. An electrical stimulation mapping investigation in 117 patients. J Neurosurg 71:316–326

Olivier A (1996) Surgical strategies for patients with supplementary sensorimotor area epilepsy. The Montreal experience. Adv Neurol 70:429–443

Ono O, Kubik S, Abernathy CD (1990) Atlas of the cerebral sulci. Atlas of the cerebral sulci. Thieme, New York

Passingham RE (1996) Functional specialization of the supplementary motor area in monkeys and humans. Adv Neurol 70:105–116

Paus T, Petrides M, Evans AC, Meyer E (1993) Role of the human anterior cingulate cortex in the control of oculomotor, manual, and speech responses: a positron emission tomography study. J Neurophysiol 70:453–469

Penfield W, Welch K (1951) The supplementary motor area of the cerebral cortex; a clinical and experimental study. AMA Arch Neurol Psychiatry 66:289–317

Pieniadz JM, Naeser MA (1984) Computed tomographic scan cerebral asymmetries and morphologic brain asymmetries. Correlation in the same cases post mortem. Arch Neurol 41:403–409

Price CJ (2000) The anatomy of language: contributions from functional neuroimaging. J Anat 197:335–359

Pugh KR, Shaywitz BA, Shaywitz SE, Constable RT, Skudlarski P, Fulbright RK et al (1996) Cerebral organization of component processes in reading. Brain 119:1221–1238

Rao SM, Binder JR, Bandettini PA, Hammeke TA, Yetkin FZ, Jesmanowicz A et al (1993) Functional magnetic resonance imaging of complex human movements. Neurology 43:2311–2318

Rizzolatti G, Luppino G, Matelli M (1996) The classic supplementary motor area is formed by two independent areas. Adv Neurol 70:45–56

Roland PE (1999) Brain activation. In: Motor functions. Language. Wiley, New York, pp 269–290

Roland PE, Larsen B, Lassen NA, Skinhoj E (1980a) Supplementary motor area and other cortical areas in organization of voluntary movements in man. J Neurophysiol 43:118–136

Roland PE, Skinhoj E, Lassen NA, Larsen B (1980b) Different cortical areas in man in organization of voluntary movements in extrapersonal space. J Neurophysiol 43:137–150

Rowe JB, Toni I, Josephs O, Frackowiak RS, Passingham RE (2000) The prefrontal cortex: response selection or maintenance within working memory? Science 288:1656–1660

Rumeau C, Tzourio N, Murayama N, Peretti-Viton P, Levrier O, Joliot M et al (1994) Location of hand function in the sensorimotor cortex: MR and functional correlation. AJNR Am J Neuroradiol 15:567–572

Schwalbe G (1881) Lehrbuch der neurologie. Verlag von Eduard Besold, Erlangen

Seitz RJ, Schlaug G, Knorr U, Steinmetz H, Tellmann L, Herzog H (1996) Neurophysiology of the human supplementary motor area. Positron emission tomography. Adv Neurol 70:167–175

Shaywitz BA, Shaywitz SE, Pugh KR, Constable RT, Skudlarski P, Fulbright RK et al (1995) Sex differences in the functional organization of the brain for language. Nature 373:607–609

Shibasaki H, Sadato N, Lyshkow H, Yonekura Y, Honda M, Nagamine T et al (1993) Both primary motor cortex and supplementary motor area play an important role in complex finger movement. Brain 116:1387–1398

Shima K, Aya K, Mushiake H, Inase M, Aizawa H, Tanji J (1991) Two movement-related foci in the primate cingulate cortex observed in signal-triggered and self-paced forelimb movements. J Neurophysiol 65:188–202

Sobel DF, Gallen CC, Schwartz BJ, Waltz TA, Copeland B, Yamada S et al (1993) Locating the central sulcus: comparison of MR anatomic and magnetoencephalographic functional methods. AJNR Am J Neuroradiol 14:915–925

Steinmetz H, Seitz RJ (1991) Functional anatomy of language processing: neuroimaging and the problem of individual variability. Neuropsychologia 29:1149–1161

Steinmetz H, Furst G, Freund HJ (1989a) Cerebral cortical localization: application and validation of the proportional grid system in MR imaging. J Comput Assist Tomogr 13:10–19

Steinmetz H, Rademacher J, Huang YX, Hefter H, Zilles K, Thron A et al (1989b) Cerebral asymmetry: MR planimetry of the human planum temporale. J Comput Assist Tomogr 13:996–1005

Steinmetz H, Ebeling U, Huang YX, Kahn T (1990a) Sulcus topography of the parietal opercular region: an anatomic and MR study. Brain Lang 38:515–533

Steinmetz H, Rademacher J, Jancke L, Huang YX, Thron A, Zilles K (1990b) Total surface of temporoparietal intrasylvian cortex: diverging left-right asymmetries. Brain Lang 39:357–372

Steinmetz H, Volkmann J, Jancke L, Freund HJ (1991) Anatomical left-right asymmetry of language-related temporal cortex is different in left- and right-handers. Ann Neurol 29:315–319

Talairach J, Tournoux P (1988) Co-planar stereotaxic atlas of the humanbrain. 3-Dimensional proportional system. An approach to cerebral imaging. Thieme, New York

Tanji J (1994) The supplementary motor area in the cerebral cortex. Neurosci Res 19:251–268

Tanji J, Shima K (1994) Role for supplementary motor area cells in planning several movements ahead. Nature 371:413–416

Tanji J, Okano K, Sato KC (1987) Relation of neurons in the nonprimary motor cortex to bilateral hand movement. Nature 327:618–620

Tanji J, Okano K, Sato KC (1988) Neuronal activity in cortical motor areas related to ipsilateral, contralateral, and bilateral digit movements of the monkey. J Neurophysiol 60:325–343

Tognola G, Vignolo LA (1980) Brain lesions associated with oral apraxia in stroke patients: a clinico-neuroradiological investigation with the CT scan. Neuropsychologia 18:257–272

Ture U, Yasargil DC, Al-Mefty O, Yasargil MG (1999) Topographic anatomy of the insular region. J Neurosurg 90:720–733

Viallet F, Massion J, Massarino R, Khalil R (1992) Coordination between posture and movement in a bimanual load lifting task: putative role of a medial frontal region including the supplementary motor area. Exp Brain Res 88:674–684

Vogt C, Vogt O (1919) Allgemeinere ergebnisse unserer hirnforschung. J Psychol Neurol 25:279–461

Vogt O, Vogt C (1926) Die vergleichend-architektonische und vergleichend-reizphysiologische felderung der grobhirnrinde unter besonderer berücksichtigung der menschilchen. Naturwissenchaften 14:1190–1194

Vogt BA, Nimchinsky EA, Vogt LJ, Hof PR (1995) Human cingulate cortex: surface features, flat maps, and cytoarchitecture. J Comp Neurol 359:490–506

Vogt BA, Vogt LJ, Nimchinsky EA (1997) Primate cingular cortex chemoarchitecture and its disruption in Alzheimer's disease. In: Bloom FE, Bjorklund A, Hokfelt T (eds) Handbook of chemical neuroanatomy, vol 13. Elsevier Science, Amsterdam, pp 455–528

von Economo C, Koskinas GN (1925) Die Cytoarchitektonik der Hirnrinde des erwachsenen Menschen. Springer, Berlin

Williams PL, Warwick R, Dyson M (1989) Grays anatomy, 37th edn. Churchill Livingstone, Edinburgh/New York, pp 1047–1063

Yasargil MG (1994) Microneurosurgery. Thieme, Stuttgart

Yoshiura T, Higano S, Rubio A, Shrier DA, Kwok WE, Iwanaga S et al (2000) Heschl and superior temporal gyri: low signal intensity of the cortex on T2-weighted MR images of the normal brain. Radiology 214:217–221

Yousry TA (1998) Historical perspective: the cerebral lobes and their boundaries. Int J Neuroradiol 4:342–348

Yousry TA, Schmid UD, Jassoy AG, Schmidt D, Eisner WE, Reulen HJ et al (1995) Topography of the cortical motor hand area: prospective study with functional MR imaging and direct motor mapping at surgery. Radiology 195:23–29

Yousry TA, Schmid UD, Schmidt D, Hagen T, Jassoy A, Reiser MF (1996) The central sulcal vein: a landmark for identification of the central sulcus using functional magnetic resonance imaging. J Neurosurg 85:608–617

Yousry TA, Fesl G, Buttner A (1997a) Heschl's Gyrus: anatomic description and methods of identification on magnetic resonance imaging. Int J Neuroradiol 3:2–12

Yousry TA, Schmid UD, Alkadhi H, Schmidt D, Peraud A, Buettner A et al (1997b) Localization of the motor hand area to a knob on the precentral gyrus. A new landmark. Brain 120:141–157

Yousry TA, Yousry I, Naidich TP (2001) Progress in neuroanatomy. In: Demaerel P (ed) Recent advances in diagnostic neuroradiology. Springer, Berlin

Zilles K, Schlaug G, Geyer S, Luppino G, Matelli M, Qu M et al (1996) Anatomy and transmitter receptors of the supplementary motor areas in the human and nonhuman primate brain. Adv Neurol 70:29–43